國立臺灣大學理學院應用物理研究所

博士論文

Graduate Institute of Applied Physics

College of Science

National Taiwan University

Doctoral Dissertation

磁性層狀碲化物之合成與電催化穩定性研究

Synthesis and Electrocatalytic Stability of Magnetic Layered Tellurides

歐姆·普拉卡什·古傑拉

Om Prakash Gujela

指導教授：謝馬利歐

Advisor: Mario Hofmann

中華民國 114 年 09 月

Sept 2025

doi:10.6342/NTU202503490

DEDICATION

This Ph.D. dissertation is dedicated to my revered father, **Shree Ram Janma Singh**, whose vision, values, and unwavering belief in the power of education ignited the spark of learning within me.

doi:10.6342/NTU202503490

doi:10.6342/NTU202503490

ACKNOWLEDGEMENTS

First and foremost, I would like to express my deepest gratitude to my advisor, **Prof. Mario Hofmann**, whose unwavering support, insightful guidance, and constant encouragement have been pivotal throughout the course of my doctoral research. Working under his mentorship has been an intellectually enriching and transformative experience—one that I will cherish for a lifetime. Prof. Hofmann not only inspired me to think like a researcher but also helped me develop the perseverance and curiosity essential for true research. I was often amazed by the clarity and simplicity with which he approached complex problems that seemed overwhelming to me. His brilliance and humility continue to be a source of inspiration. He has been much more than an advisor—serving as a mentor, guide, and friend.

I am profoundly grateful to **Dr. Raman Sankar**, Associate Research Scientist at the Institute of Physics, Academia Sinica, Taiwan, for his generous support in facilitating the synthesis of Fe_3GeTe_2 and Fe_3GaTe_2 single crystals in his laboratory. His patient guidance and willingness to teach, even the fundamentals—have been immensely valuable. I am also thankful to him for agreeing to serve on my dissertation committee and for taking a keen interest in my research. His thoughtful feedback and insightful suggestions significantly enriched the quality of this thesis.

I also wish to thank **Dr. Ya-Ping Hsieh**, Associate Research Fellow at the Institute of Atomic and Molecular Sciences, Academia Sinica, Taiwan, for her invaluable discussions and for patiently entertaining even the most elementary questions. Her openness and expertise were immensely helpful to my understanding and progress.

doi:10.6342/NTU202503490

I would also like to express my sincere gratitude to **Prof. Yang-Fang Chen**, Professor, Department of Physics, National Taiwan University, Taipei, Taiwan, and **Prof. Ding-Rui Chen**, Assistant Professor, Department of Electronics Engineering, Chung Yuan University, Taoyuan, Taiwan, for kindly consenting to serve on my Ph.D. dissertation committee. Their willingness to contribute their time, expertise, and guidance is deeply appreciated.

My sincere thanks also go to **Dr. Mukesh Kumar Pandey** and **Dr. Santhanamoorthi** for their consistent encouragement and support throughout my Ph.D. journey. I am especially indebted to my dear friend **Mr. Danish Ali**, whose steadfast support and companionship at every step of this journey have been a pillar of strength during both challenges and triumphs.

I would like to sincerely acknowledge all the members of MY Lab for fostering a collaborative and friendly environment, and for the enriching scientific discussions that have significantly contributed to both my academic and personal growth. It has been a pleasure and a privilege to be part of such a dynamic and inspiring group. I am especially grateful to **Dr. Bhartendu Papnai** for his constant motivation and guidance at every step of my journey.

Finally, and most importantly, I extend my heartfelt gratitude to my beloved mother, **Smt. Devmati Devi**, whose unwavering belief in me and continuous encouragement have been the foundation of all my academic pursuits. I owe immense thanks to my wife, **Vidhatri Gujela**, whose love, patience, and support made this journey possible. I also extend sincere thanks to my younger brother, **Dev Prakash Gujela**, and his wife, **Neha Gujela**, for their continual encouragement and support during every phase of my Ph.D. journey. I am deeply thankful to my daughter, **Advika Gujela**, for being an understanding and joyful presence, even during times when my research commitments kept me away.

doi:10.6342/NTU202503490

ABSTRACT & KEYWORDS (Chinese)

磁場輔助電催化已被視為一種有前景的方法，可提升電化學反應的動力學與選擇性，特別是在能源轉換技術中扮演核心角色的氧化反應（OER）。鐵磁性電極能夠促進自旋極化的電荷轉移與氧中間體的相互作用，從而提升催化效率。儘管如 $CoFe_2O_4$ **與 $NiZnFe_4O_x$ 等材料已展現出在磁場下增強的 OER 活性，然而同時具備強鐵磁性與高催化活性的材料卻相當稀少**。

二維（2D）層狀磁性材料因其可調控的磁性與表面特性，提供了一種獨特的解決方案。在眾多材料中，鐵碲基化合物如 Fe_3GeTe_2（FGT）與 $Fe_{3-x}GaTe_2$（FGaT）備受矚目。這些材料展現出顯著的磁各向異性、高表面反應性，以及範圍從 130 K 至超過 380 K 的居里溫度，成為磁-電催化耦合的理想候選材料。

然而，這些材料在環境與電化學條件下的穩定性尚未被充分理解。有研究指出 FGT 在空氣中會發生降解，亦有報告顯示其在操作環境中具有一定穩定性。本論文旨在探討鐵碲鐵磁材料的磁性、催化性與環境行為，以理解其降解機制，並尋求提升其在 OER 應用中操作穩定性的策略。

本研究採用一種創新的結構同系物方法，系統性地研究 FGT 催化性能的起源及其電化學降解的根本原因。透過合成並表徵 Fe_3GeTe_2 與其同構類比物 Fe_3GaTe_2（FGaT），建立一個可直接比較的研究框架，以釐清子層組成對活性與穩定性的影響。結合

doi:10.6342/NTU202503490

先進的電化學測量、表面分析技術與密度泛函理論（DFT）計算，本研究揭示電子結構對催化行為的影響，並找出造成材料降解的原子尺度因素。

研究結果顯示，FGT 與 FGaT 的催化活性主要由 Fe 的 3d 軌域所主導，這些軌域調控氧中間體在 OER 過程中的吸附與轉化。此發現解釋了兩種材料在基面上表現出相似的析氫反應（HER）與析氧反應（OER）性能。然而，在長期電化學穩定性方面，兩者表現出顯著差異：FGaT 的降解速度遠高於 FGT。透過 DFT 分析，我們將此不穩定性歸因於 Ga 取代 Ge 所導致的晶格內 Te 原子鍵結強度下降，進而促進表面重構，並在電化學條件下形成非晶或氧化相。

本研究證明了結構同系策略在解耦催化活性與電化學降解方面的潛力，並為設計穩定的磁性電催化材料提供了理性設計準則。藉由明確指出影響性能與降解的電子與結構起源，本論文為未來開發具備最佳催化效率與穩定性的次世代二維鐵磁材料奠定基礎。最終，本研究深化了對自旋相關電催化現象的基礎理解，並為可持續能源轉換技術開創了新方向。

關鍵詞：電催化；氫氣析出反應；單晶生長；鐵磁性層狀材料；循環伏安法

doi:10.6342/NTU202503490

ABSTRACT & KEYWORDS (English)

Magnetic-field-assisted electrocatalysis has emerged as a promising approach to enhance the kinetics and selectivity of electrochemical reactions, especially the oxygen evolution reaction (OER), which is central to energy conversion technologies. Ferromagnetic electrodes enable spin-polarized charge transfer and interaction with oxygen intermediates, improving catalytic performance. While materials such as $CoFe_2O_4$ and $NiZnFe_4O_x$ have shown enhanced OER activity under magnetic influence, these systems must simultaneously possess strong ferromagnetism and catalytic activity—a combination not easily found.

Two-dimensional (2D) layered magnetic materials offer a unique solution due to their tunable magnetic and surface properties. Among these, iron-telluride-based compounds like Fe_3GeTe_2 (FGT) and $Fe_{3-x}GaTe_2$ (FGaT) have attracted attention. These materials exhibit significant magnetic anisotropy, high surface reactivity, and Curie temperatures ranging from 130 K to over 380 K, making them suitable candidates for magnetic-electrocatalytic coupling.

However, the environmental and electrochemical stability of these materials remains poorly understood. Reports indicate degradation of FGT in ambient conditions, while others suggest stability under operating environments. This dissertation investigates the magnetic, catalytic, and environmental behavior of iron-telluride ferromagnets, aiming to understand their degradation mechanisms and identify strategies to enhance their operational durability in OER applications.

doi:10.6342/NTU202503490

In this thesis, we address this challenge by employing a novel structural homolog approach to systematically investigate the origins of FGT's catalytic performance and the fundamental causes of its electrochemical degradation. By synthesizing and characterizing Fe_3GeTe_2 alongside its isostructural analog Fe_3GaTe_2 (FGaT), we provide a direct comparative framework that isolates the effects of sublayer composition on both activity and stability. Using a combination of advanced electrochemical measurements, surface characterization techniques, and density functional theory (DFT) calculations, we elucidate the electronic structure contributions to catalytic behavior and identify the atomic-scale factors responsible for material deterioration.

Our results reveal that the catalytic activity of both FGT and FGaT is predominantly governed by Fe 3d orbitals, which mediate the adsorption and transformation of oxygen intermediates during OER. This finding explains the comparable basal-plane hydrogen evolution and oxygen evolution reaction performances observed experimentally for both materials. However, we find a marked difference in their long-term electrochemical stability: FGaT exhibits significantly accelerated degradation compared to FGT. Through DFT analysis, we attribute this instability to the substitution of Ga for Ge, which weakens the bonding strength of Te atoms within the lattice, thereby facilitating surface reconstruction and the formation of amorphous or oxide phases under electrochemical conditions.

These insights establish structural homologs as a powerful strategy to decouple catalytic activity from electrochemical deterioration, enabling more rational design principles for stable magnetic electrocatalysts. By pinpointing the electronic and structural origins of both performance and degradation, this work lays the foundation for engineering next-generation

doi:10.6342/NTU202503490

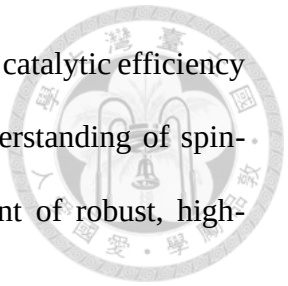

2D ferromagnetic materials with tailored compositions that optimize both catalytic efficiency and durability. Ultimately, this research advances the fundamental understanding of spin-dependent electrocatalysis and opens new avenues for the development of robust, high-performance materials for sustainable energy conversion technologies.

Keywords: electrocatalysis; hydrogen evolution reaction; single-crystal growth; ferromagnetic layered materials; cyclic voltammetry

doi:10.6342/NTU202503490

doi:10.6342/NTU202503490

Table of Contents

doi:10.6342/NTU202503490

doi:10.6342/NTU202503490

doi:10.6342/NTU202503490

doi:10.6342/NTU202503490

List of Figures

doi:10.6342/NTU202503490

doi:10.6342/NTU202503490

doi:10.6342/NTU202503490

doi:10.6342/NTU202503490

FGT case (top) and visible degradation in FGaT (bottom), consistent with surface corrosion

doi:10.6342/NTU202503490

doi:10.6342/NTU202503490

List of Tables

doi:10.6342/NTU202503490

CHAPTER: 01

INTRODUCTION

1.1 Background and Context

The twenty-first century is defined by an unprecedented escalation in global energy consumption, primarily driven by population growth, rapid industrialization, and rising standards of living in developing economies. According to the International Energy Agency (IEA), worldwide primary energy demand is projected to increase by approximately 25% between 2022 and 2050 under current policy scenarios, despite improvements in energy efficiency and greater deployment of renewable energy technologies. The overwhelming majority of today's energy supply continues to be derived from fossil fuels: oil, coal, and natural gas, which together account for approximately 80% of the global energy mix. This reliance poses severe risks to planetary health, as energy production and use are responsible for over 73% of global greenhouse gas (GHG) emissions.

The resulting accumulation of atmospheric carbon dioxide and other greenhouse gases is the principal driver of anthropogenic climate change. Recent reports from the Intergovernmental Panel on Climate Change (IPCC) warn that, unless rapid, far-reaching transitions occur across energy, land, infrastructure, and industrial systems, it will be impossible to limit global warming to 1.5°C above pre-industrial levels, a threshold widely regarded as critical to avoiding the most catastrophic effects of climate disruption. Manifestations of the climate crisis, including increased frequency and severity of extreme weather events, sea level rise, and the destabilization of vital ecosystems, highlight the urgent need to decarbonize the global energy system.

doi:10.6342/NTU202503490

Meeting rising energy demands while simultaneously reducing carbon emissions presents a grand scientific and engineering challenge. This imperative has fueled the search for sustainable energy conversion and storage technologies, capable of delivering reliable power with minimal environmental impact. Among these, advanced electrocatalytic processes are recognized as key enablers for the transition to a low-carbon, circular energy economy.

Role of electrocatalysis in sustainable energy conversion:

Electrocatalysis plays a central role in sustainable energy conversion by enabling the efficient transformation of abundant molecules such as water (H_2O), carbon dioxide (CO_2), and nitrogen (N_2) into valuable fuels and chemicals using renewable electricity. Through carefully engineered electrocatalysts, key processes, including water splitting for hydrogen production, CO_2 electroreduction to carbon-based fuels, and nitrogen reduction to ammonia, can be performed under ambient conditions, offering a pathway to decarbonized fuel and chemical synthesis [1].

For example, water electrolysis, facilitated by advanced electrocatalysts, allows the storage of intermittent solar and wind energy in the form of green hydrogen, a clean fuel that emits only water on combustion or use in fuel cells. Similarly, electrocatalytic CO_2 reduction technologies are being developed to recycle CO_2 emissions into chemicals such as ethylene, methanol, or alcohols, helping to close the carbon loop and mitigate climate change impacts [2]. Importantly, these approaches not only lower greenhouse gas emissions but also enable value-added production from waste streams or atmospheric pollutants.

doi:10.6342/NTU202503490

Ongoing research focuses on lowering the cost, improving the efficiency, and increasing the stability of electrocatalysts, especially those based on earth-abundant elements, to facilitate large-scale adoption and industrial viability [1]. Thus, by coupling renewable energy with electrocatalytic processes, it becomes possible to replace fossil-derived fuels and chemicals with sustainable alternatives, establishing electrocatalysis as a cornerstone of the clean energy transition [1].

Water splitting has gained significant attention as a promising pathway for sustainable hydrogen production, directly coupling renewable electricity to the generation of high-purity hydrogen and oxygen gases from water. This electrochemical process comprises two half-reactions: the hydrogen evolution reaction (HER) at the cathode and the oxygen evolution reaction (OER) at the anode.

The Scientific and Technological Significance of OER

The scientific and technological significance of the oxygen evolution reaction (OER) is rooted in its status as the principal kinetic bottleneck for water splitting and many related sustainable energy technologies. Thermodynamically, the OER requires overcoming a substantial free energy barrier to convert water (or hydroxide ions) into molecular oxygen, involving a four-electron, four-proton transfer pathway. The standard equilibrium potential for OER is 1.23 V versus the reversible hydrogen electrode (RHE), but significant additional overpotential is needed in both acidic and alkaline media due to sluggish reaction kinetics and the complex multi-step mechanism with several key reaction intermediates [3, 4].

doi:10.6342/NTU202503490

In acidic electrolytes (such as those used in proton exchange membrane electrolyzers), OER is the dominant source of energy loss, mainly because few catalyst materials are both active and stable under these conditions. Most transition metal oxides, for instance, are destabilized or corroded at the high anodic potentials required for OER, a consequence of intrinsic thermodynamic instability above the OER equilibrium potential; no known oxide is fully immune to this, leading to universal correlations between OER activity and catalyst degradation [3, 5]. In alkaline conditions, a wider range of earth-abundant catalysts is available, but the reaction still suffers from significant kinetic barriers and the overpotential remains substantial, due to the scaling relationships between the adsorption energies of intermediates like *OH, *O, and *OOH [6].

Kinetically, the OER comprises multiple steps with intricate electron and proton transfers, the most critical being the formation and desorption of the O–O bond. Mechanistically, sluggish kinetics arise from differences in the binding energies of surface-bound intermediates and from the difficulty of synchronizing simultaneous electron/proton transfers at each elementary step. This results in slow overall rates, demanding high driving voltages and thus reducing the round-trip efficiency of electrolyzers, fuel cells, and metal–air batteries [4, 7].

Recent mechanistic studies, including advanced modeling and experimental approaches, have revealed that optimizing OER performance requires not only minimizing overpotential but also achieving a balance between catalytic activity and catalyst stability, in both acidic and alkaline regimes, while carefully considering the fundamental thermodynamic limits imposed by the multistep electron/proton transfer and the ubiquitous tendency toward catalyst dissolution [5, 6].

doi:10.6342/NTU202503490

Material Design Challenges: Need for Earth-Abundant, Stable, and Efficient Electrocatalysts:

A major challenge in advancing the practical application of the oxygen evolution reaction (OER) lies in the development of electrocatalysts that are not only highly active but also stable and composed of earth-abundant materials. The current benchmark OER catalysts (notably IrO_2 and RuO_2) deliver exceptional activity and durability, particularly in acidic media, but are hindered by the scarcity and high cost of iridium and ruthenium, making them unsuitable for widespread adoption in large-scale electrolyzers and energy storage systems [8].

Most transition metal oxides that are earth-abundant (such as those based on Fe, Co, Ni, or Mn) show promising OER activity in alkaline environments but tend to dissolve or lose structural integrity under harsh acidic conditions prevalent in proton exchange membrane (PEM) electrolyzers. Overcoming this dissolution and ensuring prolonged electrochemical durability is a significant material [9].

Efforts to enhance catalytic activity (e.g., increasing surface area, creating defect sites, optimizing electronic structure) often come at the expense of long-term stability or vice versa. The ability to decouple these two properties by, for instance, using mixed-metal oxides or engineered nanostructures, is leading research direction [10].

Advanced design strategies, such as introducing nanoscale porosity, doping, heterostructure formation, hydrophobic supports, and defect engineering, have shown promise for

doi:10.6342/NTU202503490

optimizing the binding energies of OER intermediates, increasing the density of active sites, and enhancing the accessibility and durability of catalysts [9].

Special approaches, such as embedding active metallic centers within acid-stable matrices (e.g., using Mn to stabilize Co sites or hydrophobic supports to suppress metal oxide dissolution), have recently demonstrated breakthroughs in the field, enabling improved performance of earth-abundant catalysts in acidic regimes [10].

The requirement for large-scale, sustainable hydrogen production further emphasizes the importance of using inexpensive, non-toxic, and readily available elements in catalyst design, in contrast to precious metals [10].

Key performance metrics for HER/OER:

Key performance metrics for oxygen evolution reaction (OER) electrocatalysts are established to enable rigorous comparison of activity, efficiency, and durability, guiding both fundamental research and practical development. The principal metrics include:

Overpotential (η): The extra potential (above the thermodynamic value, typically 1.23 V vs. RHE) required to drive OER at a set current density. Lower overpotentials at benchmark current densities (commonly 10 mA cm^{-2}) indicate more efficient catalysts. Overpotential directly determines the energy efficiency of water-splitting systems and is often reported as η_{10} (overpotential at 10 mA cm^{-2}) [11].

Tafel Slope: Derived from the Tafel equation ($\eta = a + b \log j$, where j is current density), the Tafel slope (b, in mV/dec) provides insight into reaction kinetics and the OER rate-

doi:10.6342/NTU202503490

determining step. Lower Tafel slopes indicate faster and more favorable kinetics, aiding mechanistic interpretation and catalyst screening [11].

Turnover Frequency (TOF): Represents the number of O_2 molecules produced per active site per unit time, serving as a measure of intrinsic catalytic activity that is independent of catalyst loading or surface area. Accurate TOF quantification requires reliable estimation of the number of electrochemically active sites [12].

Stability (Durability): Assessed by monitoring catalytic activity (often at a fixed current or potential) over extended periods (e.g., many hours or thousands of cycles), ideally under industrially relevant harsh conditions. Degradation rates, loss in activity, or morphological changes are used to quantify stability, which is critical for practical adoption [11].

Faradaic Efficiency: The fraction of total charge passed that results in O_2 evolution (as opposed to side reactions), providing a check on selectivity and measurement accuracy [13].

1.2 Emerging Role of Magnetic Effects in Electrochemistry

The fundamentals of magnetic field effects in electrochemical systems are grounded in the interaction between magnetic fields and moving charged species within an electrolyte. When a magnetic field is applied perpendicular to the direction of ionic current in an electrochemical cell, the resulting Lorentz force acts on the ions, creating a magnetohydrodynamic (MHD) effect that alters mass transport dynamics near the electrode surface. Specifically, the Lorentz force ($F = i \times B$, where i is current density and B is magnetic field strength) can induce fluid motion in the electrolyte, leading to enhanced mixing, thinning of the diffusion layer, and increased limiting current density [14]. This improved

doi:10.6342/NTU202503490

mass transfer can accelerate electrochemical reaction rates and influence deposition processes.

Beyond mass transport, magnetic fields are also capable of modulating the spin states of electrons involved in electrochemical reactions, a phenomenon that becomes particularly relevant for reactions in which spin conservation rules or spin-dependent electron transfer steps play a role [15]. This can alter reaction pathways, affect catalytic activity, and open up possibilities for controlling selectivity and kinetics in electrocatalysis and energy storage devices [16].

Recent advances illustrate that both the intrinsic magnetic properties of electrocatalysts and the application of external magnetic fields can be strategically harnessed to enhance electrochemical performance in diverse systems, including batteries, fuel cells, and water-splitting devices [16]. While some effects, such as the MHD-driven mass transport enhancement, are relatively well understood, the influence of magnetic fields at the microscopic (e.g., spin) level remains an active and rapidly developing area of research, with ongoing efforts to clarify the mechanisms and fully exploit the potential of magneto-electrochemistry [15, 17, 18].

Spin-polarized electron transfer and spin-selective catalysis:

Spin-polarized electron transfer refers to processes in which the spin orientation of electrons, often governed by magnetic order or chirality in materials, affects the kinetics and selectivity of electrochemical reactions. In spin-selective catalysis, the alignment and polarization of

doi:10.6342/NTU202503490

electron spins at catalyst surfaces can modulate electron transfer rates and pathways, yielding enhancements unattainable by purely chemical means.

Recent studies have demonstrated that during multi-electron processes like the oxygen evolution reaction (OER), spin polarization in ferromagnetic catalysts, either induced by an external magnetic field or intrinsic magnetic order, can drive coherent spin exchange between the catalyst and reaction intermediates, accelerating the rate-determining electron transfer steps according to the principle of spin angular momentum conservation [19]. This effect is especially relevant in reactions where the final product (e.g., O_2) is a triplet state, demanding strict spin selection rules throughout the reaction mechanism.

Beyond ferromagnetic materials, electrode chirality and spin-orbit coupling in catalysts can generate spin-polarized currents inherently, as observed at chiral and topologically nontrivial surfaces, further demonstrating that spin-dependent electron transfer underpins higher efficiency and could surpass traditional activity limitations for key electrocatalytic reactions [20, 21]. Experiments also show that spin polarization at the electrode-electrolyte interface can enhance oxygen reduction and evolution activities by maintaining spin alignment in multistep charge transfer, effectively altering the reaction barrier and improving selectivity [21, 22].

The emerging field of spin-selective catalysis thus opens new possibilities for catalyst design, where manipulating electron spin, not just charge, enables fundamental advances in energy conversion processes.

doi:10.6342/NTU202503490

1.3 Literature Landscape

Recent years have witnessed rapid advances in oxygen evolution reaction (OER) catalysis, driven by the urgent demand for efficient and robust catalysts in renewable energy applications. Benchmark catalysts such as Iridium dioxide (IrO_2) and Ruthenium dioxide (RuO_2) remain the state-of-the-art due to their outstanding activity and stability, especially under acidic conditions relevant to proton exchange membrane (PEM) electrolyzers. However, drawbacks including scarcity and cost of noble metals have shifted research attention toward optimizing activity/stability through nano structuring, single-atom designs, doping, and hybridization strategies. Reviews highlight ongoing progress in the development of Ru-based OER catalysts, focusing on mechanisms, intrinsic activity, and methods to improve stability for scalable use [23, 24].

To overcome the limitations of noble metal dependence, transition metal oxides, particularly perovskites (e.g., $LaNiO_3$, $Ba_{0.5}Sr_{0.5}Co_{0.8}Fe_{0.2}O_{3-\delta}$) and spinel structures (e.g., Co_3O_4, $NiFe_2O_4$), have emerged as highly promising alternatives, especially in alkaline media, where they demonstrate excellent catalytic activity, tunable electronic structure, and improved affordability. Perovskite and spinel catalysts benefit from compositional flexibility, allowing precise tuning of lattice parameters and electronic properties for optimal OER performance. Recent reviews comprehensively summarize advances in transition metal-based materials, including the role of defect engineering, heteroatom doping, and synergistic effects to enhance both activity and durability [25, 26].

Several other studies have elucidated the role of ferromagnetism in promoting OER activity. Ren et al. demonstrated that spin-polarized oxygen adsorption on $CoFe_2O_4$ [19] surfaces

doi:10.6342/NTU202503490

enhances OER kinetics by facilitating more favorable spin alignment between the catalyst surface and oxygen intermediates, thereby lowering activation barriers and increasing reaction rates. This spin polarization effect highlights the importance of electronic spin states in catalytic processes, which can be manipulated via magnetic ordering.

Similarly, Garcés-Pineda and colleagues linked the magnetic enhancements observed in OER over $NiZnFe_4O_x$ [27] catalysts to the alignment of oxygen intermediate bonds under magnetic influence. Their work suggests that magnetic fields can induce structural and electronic rearrangements at the active sites, optimizing the adsorption geometry and strengthening the interaction with key reaction intermediates. This bond alignment mechanism provides insight into how external magnetic fields can be used to tune catalytic selectivity and efficiency.

Van der Minne et al. reported increased OER activity below the Curie temperature of $La_{0.67}Sr_{0.33}MnO_3$ [28], indicating that the presence of bulk magnetic order can couple effectively with surface catalytic sites to enhance reaction kinetics. This finding underscores the critical role of intrinsic magnetic phase transitions in modulating catalytic behavior and suggests that temperature-dependent magnetic properties can be exploited to optimize electrocatalytic performance.

Beyond these examples, ongoing research explores the integration of ferromagnetic materials with nanostructured catalysts, the influence of magnetic domain walls, and the potential synergy between magnetic and electric fields to further boost electrocatalytic reactions. The combination of advanced characterization techniques, such as spin-resolved spectroscopy and in situ magnetic measurements, with theoretical modeling continues to deepen our understanding of spin-dependent catalysis. As this field progresses, ferromagnetic electrodes

doi:10.6342/NTU202503490

are poised to play a transformative role in the design of next-generation energy conversion devices with enhanced efficiency, selectivity, and durability.

Furthermore, two-dimensional (2D) materials, notably layered double hydroxides (LDHs), transition metal dichalcogenides (TMDs), and atomically thin oxides, are at the forefront of research, thanks to their high surface-to-volume ratio and abundant active sites. The fabrication of single-atom and dual-atom catalysts embedded in 2D frameworks has led to new paradigms in OER, enabling precise tuning of local coordination and electronic environments for remarkable activity and stability [29-31]. For example, atomically dispersed transition metal centers on N-doped graphene or other 2D supports have shown the potential to outperform conventional nanoparticles in both efficiency and resource utilization.

These collective advances reflect a shift from purely empirical optimization to rational, atomic-scale engineering across IrO_2/RuO_2 benchmarks, perovskites, spinels, and 2D materials, aiming to meet future targets for sustainable and cost-effective water electrolysis and other clean energy systems [26, 32].

1.4 Importance of Transition Metal-Based Electrocatalysts

Transition metal-based electrocatalysts have emerged as crucial components in the development of efficient HER and OER systems. These materials offer several advantages over traditional noble metal catalysts, including cost-effectiveness, abundance, and potential for high catalytic activity.

doi:10.6342/NTU202503490

Iron (Fe) is particularly attractive for HER/OER applications due to its abundance, low cost, and environmental friendliness. Fe-based materials can exhibit high catalytic activity when properly engineered, making them promising alternatives to noble metals like platinum.

Abundance and Cost-Effectiveness: Iron is one of the most abundant metals in the Earth's crust, which makes it an attractive choice for large-scale applications. The use of Fe-based materials can significantly reduce the cost of electrocatalysts compared to precious metals like platinum [33, 34].

Environmental Benefits: Fe-based materials are generally more environmentally friendly than noble metals, as they are less toxic and more sustainable. This aspect is crucial for developing green energy technologies [33, 35].

Catalytic Activity: Recent advances in materials science have shown that Fe-based compounds can be engineered to exhibit high catalytic activity for the HER/OER. This is achieved through modifications in their electronic and structural properties, such as doping or alloying with other elements [34, 36].

Versatility in Composition: Fe can form a wide range of compounds with different anionic components (e.g., oxides, hydroxides, sulfides, selenides), allowing for the tuning of their catalytic properties. This versatility is beneficial for optimizing HER/OER performance under various conditions [33, 35].

doi:10.6342/NTU202503490

1.5 List of other materials are similar to those (2D ferromagnets and antiferromagnets) and have been used in electrochemistry:

$FePS_3$, FeSe, FeTe: Some compounds in this family exhibit robust 2D ferromagnetism or antiferromagnetism and have been explored for electrocatalytic HER and OER due to their tunable electronic structure and active edge sites [37-40].

MoS_2, WS_2, $MoSe_2$, WSe_2: While these TMDs are best known for their electronic and catalytic properties, some doped or modified TMDs (e.g., Fe- or V-doped) show magnetic ordering and are widely used in electrochemistry, notably for HER and CO_2 reduction, utilizing their exposed edge sites for enhanced catalytic activity [37, 40].

VA-$Mo_{1-x}M_xS_2$ (M = Nb, Ta): Doped variants have improved catalytic performance in CO_2 reduction, and variable edge chemistry can promote both charge transfer and catalytic efficiency [40].

$MnPS_3$, $NiPS_3$: These antiferromagnetic materials have been studied as 2D electrocatalysts and for applications in batteries and supercapacitors, exploiting their layer-dependent magnetic and electronic properties [38, 39].

CrI_3, $Cr_2Ge_2Te_6$: These are prototypical 2D ferromagnets; their use has been extended to electrochemical sensing, with potential catalytic function owing to their surface structure and tunable magnetic state [38, 39].

While classic antiferromagnets like NiO, MnO_2, and Co_3O_4 are frequently used in electrochemistry, several layered/ferrimagnetic or ferrimagnetic oxides, such as Fe_2O_3

doi:10.6342/NTU202503490

nanosheets and heterostructures that exploit spin ordering and anisotropy, are being explored for OER and HER [38, 41].

Borophene, Bismuthene: Though not magnetic themselves, they exemplify how 2D sheets with tunable edge, defect, or doping-induced magnetism can yield materials effective for energy conversion and sensing [41].

2D Ferroelectric/Ferromagnetic Metals (e.g., $CuCrP_2S_6$, Fe_3Sn_2): These combine ferromagnetic or multiferroic order with electrical polarization, supporting spintronic and electrochemical synergies [42-44].

Table 1.1: Representative 2D magnets used in electrochemistry

Material	Magnetic Order	Electrochemical Role	References
$FePS_3$, $MnPS_3$	Ferromagnet	OER, HER, Spin-polarized catalysis	[38, 39]
MoS_2, $MoSe_2$, WS_2	Antiferromagnet	Water splitting, batteries, supercapacitor	[37, 38, 40]
CrI_3, $Cr_2Ge_2Te_6$	(Doped) Magnet	HER, CO_2RR, OER (edge, defect driven)	[38, 39]
Borophene, Bismuthene	Ferromagnet	Electrochemical sensing, basic study	[41]

doi:10.6342/NTU202503490

Material Requirements and the Promise of Iron-Telluride-Based Electrocatalysts:

These results demonstrate the significant potential of ferromagnetic electrodes for enhancing the oxygen evolution reaction (OER), yet they also reveal a fundamental challenge in the design of such materials. To be effective, electrodes must simultaneously satisfy two critical and often competing requirements: they must exhibit robust ferromagnetism to enable magnetic-field coupling effects, and they must possess intrinsically high catalytic activity to drive the OER efficiently. Achieving this balance is nontrivial, as many ferromagnetic materials lack sufficient catalytic performance, while highly active catalysts often do not exhibit strong magnetic ordering.

Iron-telluride-based compounds, particularly Fe_3GeTe_2 (FGT), have recently emerged as promising candidates that inherently fulfill both criteria. FGT is a layered van der Waals ferromagnet known for its robust and tunable ferromagnetic properties, including a relatively high Curie temperature and strong magnetic anisotropy, which are advantageous for stable magnetic coupling under operating conditions. Concurrently, recent theoretical investigations have highlighted the exceptional catalytic activity of FGT surface sites toward the OER, attributing this to favorable electronic structures and optimal adsorption energies for key oxygen intermediates. These studies suggest that FGT not only maintains strong spin polarization but also provides active sites that facilitate the multi-electron transfer steps required for efficient oxygen evolution [45].

Moreover, the unique two-dimensional nature of FGT enables facile engineering of its surface properties through exfoliation, doping, or heterostructure formation, opening avenues to further optimize both its magnetic and catalytic functionalities. This dual capability

doi:10.6342/NTU202503490

positions Fe_3GeTe_2 as a compelling platform for exploring spin-dependent electrocatalysis and developing next-generation magnetic electrocatalysts that overcome the traditional trade-offs between magnetism and catalytic activity.

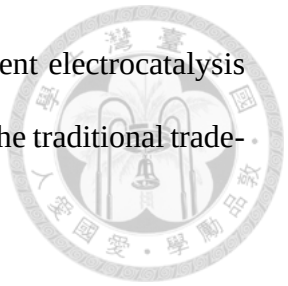

Magnetization Measurements of Fe_3GeTe_2 (FGT)

Iron germanium telluride (Fe_3GeTe_2, or FGT) is a quasi-two-dimensional (2D) van der Waals ferromagnet featuring tunable electronic and magnetic properties, positioning it as a promising candidate for spintronics and electrocatalysis applications [46-48]. A central technique for probing its ferromagnetic character is the use of isothermal field-dependent magnetization (M–H curve) measurements, which elucidate how magnetization responds to external magnetic fields at various temperatures. These curves provide critical insights into properties such as coercivity, remanent magnetization, saturation magnetization, and Curie temperature. Recent studies have further sought to relate these magnetic features to catalytic oxygen evolution reaction (OER) activity, emphasizing how spin polarization and magnetic ordering impact catalytic performance.

Isothermal Magnetization and Magnetic Anisotropy

Detailed M–H measurements have revealed FGT's pronounced magnetic anisotropy and critical behavior. For example, Mondal and Roy [49] examined CVT-grown Fe_3GeTe_2 single crystals and observed strong anisotropic ferromagnetism between in-plane (ab) and out-of-plane (c-axis) directions. At low temperatures (e.g., 2K), well-defined coercivity and saturation are visible in M–H curves, indicative of robust ferromagnetic domains. As the temperature approaches the Curie temperature (~220–230 K), hysteresis loops narrow and the saturation magnetization decreases. Critical behavior analysis demonstrates that FGT

doi:10.6342/NTU202503490

follows a three-dimensional Ising model, with reported critical exponents $\beta \approx 0.31$ and $\gamma \approx 1.25$. These results highlight FGT's robust ferromagnetism and strong uniaxial anisotropy, a hallmark of its layered crystal structure.

Thickness-Dependent Magnetic Transitions

The number of FGT layers markedly influences its magnetic properties. R. Roemer et al. [50] investigated monolayer, bilayer, and multilayer FGT systems, showing that monolayer FGT exhibits a reduced Curie temperature (~130 K) compared to the bulk value (~220 K). Their M–H analysis revealed layer-dependent coercivity and spin-transition behaviors, as well as a transition from metallic to semi-metallic electronic character with decreasing layer thickness. These findings are consistent with previous reports on the suppression of magnetism and modification of electronic band structure in atomically thin FGT.

Spin-Dependent Electron Transfer in OER

Li et al. (2024) developed van der Waals heterostructures comprising Fe_3GeTe_2 (FGT) and hexagonal boron nitride (h-BN) to investigate their performance in the oxygen evolution reaction (OER). Their study revealed that spin-aligned electrons originating from FGT substantially enhance spin-selective charge transfer processes at the FGT/h-BN interface, thereby improving the electrocatalytic activity. To establish the relationship between the magnetic state and catalytic performance, the authors systematically employed M–H loop measurements at various temperatures alongside electrochemical impedance spectroscopy, demonstrating a strong correlation between the magnetization of FGT and its OER activity [51].

doi:10.6342/NTU202503490

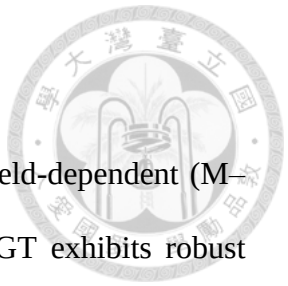

Temperature-Dependent Ferromagnetism

Temperature-dependent magnetization measurements, including both field-dependent (M–H) and temperature-dependent (M–T) curves, have established that FGT exhibits robust ferromagnetic order across a wide range of thicknesses. It was shown that the Curie temperature (T_c), which defines the transition from the ferromagnetic to the paramagnetic phase, can be effectively modulated by sample thickness: monolayer FGT displays a T_c around 130 K, while bulk crystals reach up to approximately 220 K. In all cases, the saturation magnetization increases as temperature decreases, and sharp hysteresis loops are observed, confirming strong ferromagnetism even in atomically thin layer [47].

Isothermal Field-Dependent Magnetization (M–H Curves)

Detailed isothermal M–H measurements at various temperatures reveal square-shaped hysteresis loops at low temperatures, a hallmark of strong ferromagnets with high coercivity (0.3–0.6 T). Both the remanent magnetization and coercivity decrease with increasing temperature, and the curves illustrate the clear transition from ferromagnetic to paramagnetic states as the temperature approaches T_c [46].

Magnetization Measurements of Fe_3GaTe_2 (FGaT)

Fe_3GaTe_2 is an emerging layered van der Waals ferromagnetic material, structurally analogous to the well-studied Fe_3GeTe_2, but distinct for its tunable composition and pronounced magnetic anisotropy, which make it a prospective candidate for both magnetoelectronic and electrocatalytic applications, including the oxygen evolution reaction (OER). Characterization by temperature-dependent isothermal magnetization (M–H) curves

doi:10.6342/NTU202503490

is crucial for probing its magnetic phase transitions, anisotropy, magnetocaloric effect, and for establishing possible links between these magnetic phenomena and its functionality in electrochemical systems.

Room-Temperature Ferromagnetism and Critical Behavior

Recent studies have established that Fe_3GaTe_2 exhibits robust ferromagnetism well above room temperature. Algaidi et al. [52] conducted comprehensive magnetization measurements on high-quality Fe_3GaTe_2 crystals, reporting M–H curves over a broad range of temperatures (2–354 K). Their results demonstrate prominent magnetic hysteresis and coercivity under both in-plane and out-of-plane field orientations, with remarkably strong magnetic anisotropy, magnetization saturates more rapidly along the crystallographic c-axis, pointing to a preferential spin alignment. Importantly, these investigations place the Curie temperature (T_C) near 380 K, which is among the highest for van der Waals ferromagnets and underscores Fe_3GaTe_2's promise for ambient-condition spintronic devices. Detailed analysis of critical exponents ($\beta \approx 0.32$, $\gamma \approx 1.27$) suggests the material follows a three-dimensional Ising universality class. The persistence of ferromagnetic order and spin anisotropy at high temperature make Fe_3GaTe_2 especially promising for applications involving spin-polarized charge transfer, such as catalysis and magneto-transport.

Anisotropic Magnetocaloric Effect and Off-Stoichiometric Behavior

Further insights have been obtained by examining the magnetocaloric properties of $Fe_{3-x}GaTe_2$. You et al. [53] measured M–H isotherms across 2–350 K and under fields up to 7T, focusing on off-stoichiometric compositions. Their work demonstrates a significant, highly

doi:10.6342/NTU202503490

anisotropic magnetocaloric effect (MCE), with the magnetic entropy change (ΔS_m) peaking along the c-axis ($\Delta S_m \approx 3.7$ J/kg·K at ~320 K for $\Delta H = 5$ T). This anisotropy is attributed to competing exchange interactions between Fe atoms occupying different lattice sites. As off-stoichiometry increases (i.e., larger x in $Fe_{3-x}GaTe_2$), the material undergoes magnetic softening, evident as reduced coercivity and altered critical parameters. These findings indicate the tunability of the magnetic and magnetocaloric response, potentially useful for magnetic refrigeration and magneto-electrochemical applications.

Environmental Stability Challenges of Non-Oxide Ferromagnetic Electrocatalysts:

However, an underappreciated and critical issue concerning non-oxide ferromagnets such as Fe_3GeTe_2 (FGT) is their environmental stability, which remains an open and unresolved question. Several studies have reported the deterioration of FGT under ambient conditions, where exposure to air and moisture leads to the formation of complex iron oxides and hydroxides, as well as the development of amorphous surface layers that can significantly alter the material's structural and magnetic properties [50, 54-56]. This degradation not only compromises the intrinsic ferromagnetism but also potentially diminishes the catalytic activity by modifying or passivating the active sites.

In contrast, other investigations have demonstrated the electrochemical stability of transition metal tellurides [57] more broadly, highlighting their resilience under harsh reaction conditions and their promising performance as OER catalysts [58]. These conflicting reports underscore a notable discrepancy in the literature regarding the stability of telluride-based ferromagnets during electrochemical operation. Despite the growing interest in FGT for spin-dependent electrocatalysis, prior electrochemical studies have largely overlooked

doi:10.6342/NTU202503490

comprehensive assessments of its operational stability, including the mechanisms and kinetics of degradation under realistic OER conditions.

Moreover, no systematic strategies have yet been proposed or tested to mitigate such degradation, such as surface passivation, protective coatings, or electrolyte optimization. Addressing these gaps is essential to fully realize the potential of FGT and related materials in practical energy conversion devices. A thorough understanding of the interplay between environmental exposure, electrochemical conditions, and material stability will enable the rational design of durable ferromagnetic electrodes that maintain both magnetic and catalytic functionalities over extended operational lifetimes.

Homologs in Materials Research

Homologs are materials that belong to the same family or series, sharing an identical or nearly identical crystal structure but differing by a systematic variation, such as the replacement of one element with another. This concept provides a powerful framework for establishing clear structure, property relationships, since the overall lattice symmetry and bonding network are preserved while subtle compositional changes tune the electronic, magnetic, or catalytic properties. In the present study, we focus on Fe_3GeTe_2 (FGT) and Fe_3GaTe_2 (FGaT), two layered transition-metal tellurides that are isostructural, hexagonal, and ferromagnetic, but differ by the replacement of the Ge sublayer with Ga. This substitution leads to differences in Curie temperature and stability, offering a unique opportunity to decouple catalytic activity from long-term electrochemical robustness.

doi:10.6342/NTU202503490

The value of homolog studies has been extensively demonstrated in other material families. In transition-metal oxides, for example, systematic substitutions in perovskite ABO_3 structures have been shown to strongly influence oxygen electrocatalysis, establishing design principles for activity and stability in fuel cell and metal–air battery applications [59]. Likewise, layered dichalcogenides such as MoS_2, $MoSe_2$, and $MoTe_2$ provide a homolog series where chalcogen substitution alters interlayer coupling, bandgap, and catalytic efficiency, making them a model system for understanding how compositional tuning impacts electronic and electrochemical behavior[60]. More recently, detailed electrochemical studies have revealed how such homolog substitutions in two-dimensional chalcogenides influence charge transfer and catalytic kinetics, further confirming the systematic nature of these effects [61].

Building on these established approaches, the comparison between FGT and FGaT represents a novel homolog study within the class of magnetic layered electrocatalysts. Their structural similarity ensures that any differences in catalytic activity or degradation pathways can be attributed primarily to the sublayer substitution (Ge → Ga), rather than to unrelated structural variations. This makes the homolog strategy particularly useful for disentangling intrinsic catalytic behavior from extrinsic stability factors, thereby providing new insights into the design of stable, high-performance magnetic electrocatalysts.

1.6 Motivation for the Study

While Fe_3GaTe_2 and Fe_3GeTe_2 are structurally similar van der Waals materials, critical differences in their electronic and magnetic properties remain underexplored in the context of the hydrogen evolution reaction (HER). Recent studies highlight that Fe_3GaTe_2 exhibits

doi:10.6342/NTU202503490

above-room-temperature ferromagnetism (Curie temperature, T_c = 350–380 K) and strong perpendicular anisotropy, attributed to robust in-plane ferromagnetic couplings mediated by Ga atoms. In contrast, Fe_3GeTe_2 shows weaker magnetic exchange interactions and lower T_c, with antiferromagnetic tendencies in certain couplings. These disparities suggest divergent electronic structures that could influence catalytic activity, yet no systematic comparison of their HER/OER performance exists in the literature [62].

A key research gap lies in understanding how the Ga vs. Ge substitution affects charge transfer kinetics, active site accessibility, and stability under electrochemical conditions. For instance, Fe_3GaTe_2's enhanced stability in monolayer form may correlate with improved durability during HER, but this hypothesis remains untested [62].

1.7 Problem Statement

Magnetic two-dimensional (2D) materials, particularly layered ferromagnets such as Fe_3GeTe_2 (FGT), have emerged as promising candidates for next-generation electrocatalysts due to their intrinsic ferromagnetism and predicted high catalytic activity [63, 64]. These materials are anticipated to facilitate spin-polarized reaction pathways, thereby enhancing both the efficiency and selectivity of electrochemical processes [63-65]. However, a critical and unresolved challenge persists: the electrochemical and environmental instability of non-oxide ferromagnetic materials, including FGT, which significantly impedes their practical application.

Recent studies have reported the rapid degradation of FGT under ambient and electrochemical conditions, characterized by the formation of iron oxides and amorphous

doi:10.6342/NTU202503490

surface layers. While certain transition metal tellurides have demonstrated promising oxygen evolution reaction (OER) performance, inconsistencies in reported stability data and a lack of mechanistic understanding have limited their deployment. Notably, prior research has often neglected the long-term operational stability of FGT and has rarely proposed systematic strategies to mitigate its degradation.

This gap is further exacerbated by a broader challenge in the field: the simultaneous optimization of catalytic activity and long-term stability in ferromagnetic electrocatalysts, two interdependent properties that are difficult to balance [63, 66]. Without a comprehensive understanding of how atomic composition and crystal structure influence both performance and durability, the rational design of robust, high-efficiency magnetic electrocatalysts remains elusive [65, 66].

Therefore, a deeper investigation is urgently required to elucidate the origins of catalytic activity and the mechanisms underlying degradation in these materials. This research addresses this need by employing a structural homolog approach, using Fe_3GaTe_2 (FGaT) as an isostructural analog to FGT, to systematically isolate the effects of sublayer composition and bonding on electrochemical behavior. By decoupling catalytic activity from stability, this study aims to establish new design principles for engineering magnetic 2D materials with enhanced durability for sustainable energy conversion technologies.

1.8 Research Objectives

The main goal of this research is to understand and decouple the relationship between catalytic activity and electrochemical stability in magnetic two-dimensional (2D) ferromagnetic materials, particularly Fe_3GeTe_2 (FGT) and Fe_3GaTe_2 (FGaT), for their

doi:10.6342/NTU202503490

application in energy conversion technologies. To achieve this, the study focuses on the use of structural homologs to probe the fundamental mechanisms governing performance and degradation.

Specific Objectives:

1 To synthesize and characterize high-quality single crystals of Fe_3GeTe_2 (FGT) and its structural analog Fe_3GaTe_2 (FGaT), allowing a controlled comparison of their electrochemical and physical properties.

2 To evaluate and compare the electrocatalytic performance of FGT and FGaT toward the hydrogen evolution reaction (HER) with a focus on basal-plane activity.

3 To investigate the role of Fe orbitals in determining catalytic behavior, using experimental electrochemical measurements and theoretical modeling (Density Functional Theory, DFT).

4 To identify the atomic-level mechanisms that contribute to electrochemical degradation, particularly the influence of Ga substitution for Ge on lattice bonding and surface stability.

5 To demonstrate the structural homolog approach as a strategy to decouple catalytic activity from electrochemical instability, providing a framework to evaluate and design robust ferromagnetic electrocatalysts.

6 To develop fundamental design principles for next-generation magnetic 2D materials that optimize both catalytic efficiency and long-term durability under electrochemical conditions.

doi:10.6342/NTU202503490

1.9 Research Questions

1 What are the electronic and structural factors that govern the catalytic activity of Fe_3GeTe_2 (FGT) and its isostructural analog Fe_3GaTe_2 (FGaT)?

2 How does the substitution of Ge with Ga in the sublayer affect the electrochemical stability and degradation mechanisms of these layered ferromagnetic materials?

3 Can the structural homolog approach be used to decouple catalytic activity from electrochemical degradation in magnetic electrocatalysts?

4 What is the role of Fe, 3d orbitals in mediating the electrocatalytic performance during HER and OER processes?

5 What are the atomic-level origins of the instability observed in non-oxide ferromagnetic materials under electrochemical conditions?

1.10 Hypotheses

1 The catalytic activity of both Fe_3GeTe_2 and Fe_3GaTe_2 is primarily governed by Fe, 3d orbitals, which are responsible for mediating the adsorption and transformation of oxygen and hydrogen intermediates during OER and HER.

2 Substitution of Ge with Ga weakens the bonding strength of Te atoms in the crystal lattice, making Fe_3GaTe_2 more prone to electrochemical degradation compared to Fe_3GeTe_2.

3 Despite their structural similarity, FGT and FGaT exhibit decoupled behaviors in activity and stability, indicating that electronic factors (rather than only geometric ones) are critical in defining long-term performance.

doi:10.6342/NTU202503490

4 The structural homolog approach is an effective strategy for isolating the influence of atomic substitutions on the electrochemical performance and offers a rational framework for designing stable ferromagnetic electrocatalysts.

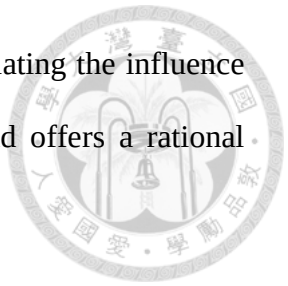

1.11 Structure of the Dissertation

This dissertation is structured into four chapters. **Chapter 1** presents the introduction, including the background of the study, motivation, problem statement, research objectives, questions, and hypotheses. **Chapter 2** details the synthesis and structural characterization of single crystals of Fe_3GaTe_2 and Fe_3GeTe_2, grown using the chemical vapor transport (CVT) method. **Chapter 3** focuses on the electrochemical performance of both materials in the hydrogen evolution reaction (HER), evaluating their activity and stability using experimental techniques. **Chapter 4** concludes the dissertation by summarizing the main findings and proposing directions for future research aimed at improving the design of stable and efficient magnetic electrocatalysts.

1.12 Limitations of the Study

While this dissertation provides detailed insights into the electrocatalytic behavior and degradation mechanisms of Fe_3GaTe_2 and Fe_3GeTe_2, it is important to acknowledge certain limitations. The experimental investigations were limited to the hydrogen evolution reaction (HER); although oxygen evolution reaction (OER) was discussed in the context of theoretical predictions and prior literature, no direct OER measurements were conducted. Furthermore, the electrocatalytic performance of the materials was not examined under the influence of an external magnetic field, despite the known significance of spin-polarized pathways in

doi:10.6342/NTU202503490

ferromagnetic systems. As a result, the potential enhancement effects of magnetic-field-assisted catalysis remain unexplored within the scope of this work. These aspects present valuable opportunities for future studies aiming to fully exploit the spintronic and electrocatalytic functionalities of magnetic 2D materials.

doi:10.6342/NTU202503490

doi:10.6342/NTU202503490

CHAPTER: 02

SINGLE CRYSTAL GROWTH OF Fe_3GeTe_2 AND Fe_3GaTe_2 USING CHEMICAL VAPOR TRANSPORT (CVT)

2.1 Introduction to CVT Method

a. Principles of the CVT Technique

The Chemical Vapor Transport (CVT) method is a widely used technique for growing high-quality single crystals by leveraging vapor-phase transport and supersaturation principles. This process involves the transport of a material in its gaseous phase from a source region to a deposition region, driven by a temperature gradient within a sealed ampoule. The method is particularly effective for materials with low natural vapor pressures, as it uses a transport agent to facilitate volatilization and subsequent crystallization.

Vapor-Phase Transport: In the CVT process, the source material reacts with a transport agent, commonly halogens or halogen compounds such as iodine or bromine, to form volatile intermediates. These gaseous species travel through the ampoule via convection and diffusion toward a cooler region, where they decompose, releasing the transport agent back into the gas phase and depositing the target material as single crystals. This cyclical reaction ensures continuous transport and deposition of material [67, 68].

Role of Supersaturation: Crystal growth in CVT is governed by supersaturation, which is achieved when the concentration of gaseous species in the deposition zone exceeds their equilibrium solubility at that temperature. By carefully controlling the temperature gradient and reaction kinetics, supersaturation can be maintained at optimal levels, promoting uniform crystal growth without excessive nucleation or defect formation [69]. For example,

doi:10.6342/NTU202503490

oscillating temperature profiles have been used to fine-tune supersaturation levels, resulting in improved crystal quality [69].

Thermodynamic Control: The CVT process is fundamentally governed by thermodynamic principles, particularly Gibbs free energy changes. For endothermic reactions, transport occurs from hotter to cooler zones, while exothermic reactions favor transport in the opposite direction. If the reaction is excessively exothermic or endothermic, the efficiency of transport may be hindered, requiring precise optimization of reaction conditions [67].

b. Advantages of the CVT Method Over Other Growth Techniques

The Chemical Vapor Transport (CVT) method offers distinct advantages over other crystal growth techniques, such as the Bridgman, flux, and floating zone (FZ) methods. These advantages make CVT particularly suitable for producing high-quality single crystals with minimal defects and tailored properties. Below is a comparison highlighting its strengths:

High Purity and Defect-Free Crystals: The CVT method operates in a sealed ampoule, minimizing contamination from external sources, unlike the Bridgman or flux methods, where impurities from the crucible or flux material can be incorporated into the crystal lattice. This makes CVT ideal for growing impurity-free crystals required for precise structural and electronic studies [67].

The absence of a molten phase during transport reduces strain-induced defects, which are common in flux-based methods [70].

Suitability for Complex Materials: CVT is highly versatile and effective for growing a wide range of materials, including intermetallic, chalcogenides, pnictides, and oxides. This

doi:10.6342/NTU202503490

versatility contrasts with methods like FZ, which are better suited for materials that can sustain high melting points without decomposition [67, 68].

For example, CVT has been successfully used to grow RuS_2 and $CuGaS_2$ crystals with excellent stoichiometric control and structural integrity [68].

Lower Growth Temperatures: Unlike the Bridgman or FZ techniques that require extremely high temperatures to maintain molten zones, CVT operates at significantly lower temperatures by utilizing volatile transport agents to facilitate material transport in the vapor phase. This reduces thermal stresses on the crystal and enhances structural integrity.

Precise Control of Growth Parameters: The use of transport agents in CVT allows fine control over growth parameters such as temperature gradients, vapor pressure, and mass transport rates. This level of precision is difficult to achieve in flux or Bridgman methods, where growth conditions are often less tunable.

Thermodynamic modeling of CVT reactions enables prediction of optimal conditions for specific materials, further enhancing reproducibility and scalability [68, 70].

Scalability and Reproducibility: CVT is well-suited for producing large single crystals with consistent quality across multiple growth cycles. In contrast, flux methods often face challenges in scaling up due to issues like flux retention or uneven crystallization [67, 71].

Tailored Morphology and Orientation: The ability to control deposition zones through temperature gradients in CVT ensures uniform crystal morphology and preferred crystallographic orientations. Such control is harder to achieve in floating zone methods due to the dynamic nature of molten zones [70].

c. Role of Transport Agents and Temperature Gradients in CVT

doi:10.6342/NTU202503490

The Chemical Vapor Transport (CVT) method relies critically on the interplay between transport agents and temperature gradients to achieve high-quality crystal growth. These two components are fundamental to the volatilization, transport, and deposition processes central to CVT.

Transport Agents

Transport agents are gaseous reactants that facilitate the volatilization of non-volatile source materials by forming volatile intermediates. These intermediates decompose in the deposition zone, releasing the transport agent and depositing the target material as crystals. The role of transport agents is essential for several reasons:

Volatilization of Non-Volatile Solids: Many materials used in CVT are non-volatile under standard conditions. Transport agents, such as halogens (e.g., iodine, bromine) or halogen compounds (e.g., $TaCl_5$), react with the source material to form volatile species. For example, iodine is commonly used for transition metal dichalcogenides like $TiSe_2$ and $MoSe_2$, enabling their efficient transport in the vapor phase [68, 70, 72].

Thermodynamic Control: The choice of transport agent is dictated by thermodynamic considerations, including the free energy of the reaction between the agent and the source material. The reaction must strike a balance: it should neither be too exothermic nor too endothermic, as extreme reactions can prevent effective transport. For instance, iodine is preferred for its moderate reactivity, which ensures efficient transport while maintaining crystal quality [68].

Material-Specific Optimization: Different materials require specific transport agents for optimal growth. For example, $TaCl_5$ has been shown to selectively grow polymorphs of TaS_2

doi:10.6342/NTU202503490

and $TaSe_2$ by tuning reaction conditions such as temperature and halogen ratios [72]. This highlights the importance of tailoring transport agents to match the chemical nature of the source material.

Temperature Gradients

Temperature gradients are another critical factor in CVT, as they drive the directional transport of volatile species from the source zone to the deposition zone:

Driving Force for Transport: A two-zone furnace is typically used in CVT setups, with a higher temperature in the source zone (T_2) and a lower temperature in the deposition zone (T_1). This gradient creates a thermodynamic driving force for vapor-phase transport via convection and diffusion.

Control of Reaction Direction: The direction of material transport in chemical vapor transport (CVT) is determined by whether the reaction between the source material and the transport agent is endothermic or exothermic. In the case of endothermic reactions, such as the transport of MoS_2 with H_2O, the material migrates from the hot zone to the cold zone. Conversely, for exothermic reactions, the transport proceeds from the cold zone to the hot zone. Careful adjustment of the temperature gradient between T_2 and T_1 is therefore essential, as it ensures efficient mass transfer and minimizes the likelihood of undesired side reactions that could compromise the purity or yield of the synthesized crystals.

Optimization of Crystal Quality: The magnitude of the temperature gradient influences supersaturation levels in the deposition zone. A steep gradient can increase nucleation density

doi:10.6342/NTU202503490

but may lead to smaller or defective crystals. Conversely, a gentler gradient promotes slower growth, resulting in larger, well-ordered crystals.

Material-Specific Adjustments: Temperature gradients must be optimized for each chemical system based on its thermodynamic properties. For example, transition metal dichalcogenides like $MoSe_2$ require carefully adjusted gradients to balance nucleation and growth rates.

Interplay Between Transport Agents and Temperature Gradients

The efficiency and quality of crystal growth in chemical vapor transport (CVT) are strongly influenced by the interplay between transport agents and temperature gradients. Transport agents facilitate volatilization by forming intermediate species that remain stable at the higher temperature zone (T_2) but decompose at the lower temperature zone (T_1), thereby enabling directional mass transfer. At the same time, the applied temperature gradient provides the thermodynamic driving force for this transfer while regulating the degree of supersaturation, which is critical for promoting uniform crystal growth. Together, these factors ensure that mass transport occurs in a controlled manner, minimizing defects and optimizing the crystallinity of the synthesized material.

2.2 Growth Parameters and Experimental Setup

a. Source of Fe, Ga, Ge, Te

The starting materials for growing Fe_3GaTe_2 and Fe_3GeTe_2 single crystals must be of high purity to ensure the structural and compositional integrity of the resulting crystals. Typical sources and purities for these materials are as follows:

doi:10.6342/NTU202503490

Iron (Fe): High-purity iron powder or granules with a purity level of 99.99% or higher are commonly used to minimize contamination from impurities such as oxygen or carbon.

Gallium (Ga): Gallium metal with a purity of at least 99.999% (5N) is preferred to prevent the introduction of trace impurities that could alter the stoichiometry of the final crystal.

Germanium (Ge): Germanium is typically sourced as high-purity ingots or powder with a purity level of 99.999% or higher to ensure precise stoichiometric control.

Tellurium (Te): Tellurium is acquired in lump or powder form with a purity level of 99.999% to avoid contamination from elements like sulfur or selenium, which can affect the crystal's properties.

b. Preparation

The preparation process for these starting materials involves several critical steps to ensure their suitability for use in the CVT method:

Weighing and Mixing: The starting materials are weighed in stoichiometric proportions based on the target composition (e.g., Fe_3GaTe_2 or Fe_3GeTe_2). The materials are mixed thoroughly in an inert environment, a glove box filled with Nitrogen, to prevent oxidation or contamination during handling [68, 73].

Figure 02.01: Mortar and pestle utilized for material mixing and grinding

doi:10.6342/NTU202503490

Figure 02.02: Inert atmosphere glove box used during material processing

Sealing in Ampoules: The prepared mixture is sealed in quartz tube with the transport agent. This step ensures that no external contaminants interfere during the CVT process [68].

Figure 02.03: System used for making and sealing quartz tubes

doi:10.6342/NTU202503490

Single Crystal Growth of Fe_3GeTe_2:

The single crystal growth of Fe_3GeTe_2 follows a two-stage synthesis process combining solid-state reaction and chemical vapor transport (CVT) [48, 74].

Polycrystalline Synthesis Stoichiometric ratios of Fe, Ge, and Te powders were mixed in a nitrogen-filled glovebox to prevent oxidation. The mixture was sealed in a small quartz tube (11 cm length, 18 mm diameter) within a larger evacuated quartz tube (31 cm length, 22 mm diameter) and heated at 650°C for 24 hours to form polycrystalline Fe_3GeTe_2. Phase purity was confirmed via X-ray diffraction (XRD).

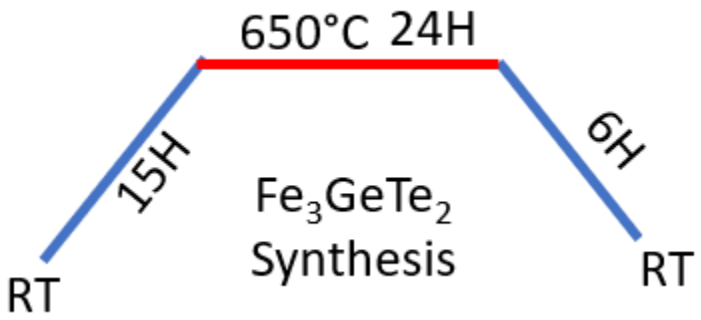

Figure 02.04: Temperature–time profile used in the synthesis of Fe_3GeTe_2

Single Crystal Growth The polycrystalline powder was reground in the glovebox, combined with 200 mg iodine (transport agent), and resealed in a growth ampoule (41 cm length, 22 mm diameter). The ampoule was placed in a dual-zone CVT furnace with a temperature gradient: 750°C (hot zone) and 650°C (cold zone). After 200 hours, hexagonal Fe_3GeTe_2 single crystals formed in the cooler region, as verified by XRD [74].

doi:10.6342/NTU202503490

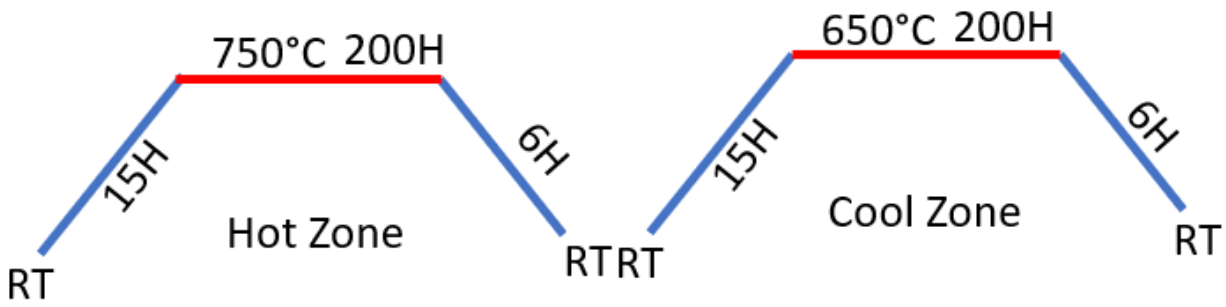

Figure 02.05: Temperature–time profile used in the single crystal growth of Fe_3GeTe_2

Figure 02.06: Small quartz tube placed inside a sealed larger tube, shown before and after crystal growth

Single Crystal Growth of Fe_3GaTe_2

The single-crystal growth of Fe_3GaTe_2 was achieved through a multi-step synthesis process that combined solid-state reactions with chemical vapor transport (CVT), adhering to established protocols for transition metal chalcogenides. The synthesis began with the preparation of GaTe precursor. Gallium (Ga) and tellurium (Te) powders were thoroughly mixed in their stoichiometric ratio and loaded into a small quartz tube (11 cm in length, 18

doi:10.6342/NTU202503490

mm in diameter) within a nitrogen-filled glove box. This small tube was then nested inside a larger quartz tube (31 cm in length, 22 mm in diameter). The outer tube was evacuated and sealed under vacuum to maintain an inert atmosphere and prevent contamination. The assembly was heated in a furnace at 600 °C for 24 hours. After cooling to room temperature, the resulting product was characterized via X-ray diffraction (XRD), confirming the successful formation of polycrystalline GaTe [75, 76].

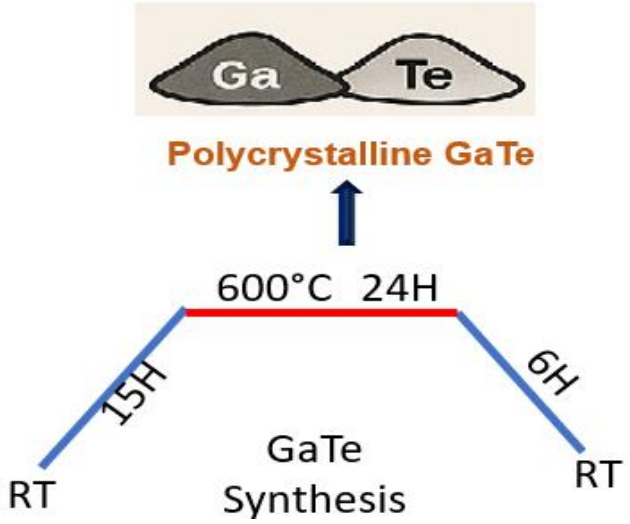

Figure 02.07: Temperature–time profile used in the synthesis of GaTe

For the synthesis of polycrystalline Fe_3GaTe_2, the prepared GaTe was ground into a fine powder using a mortar and pestle. This powder was then mixed with iron (Fe) and tellurium (Te) powders in the appropriate stoichiometric proportions corresponding to Fe_3GaTe_2. The mixture was transferred into a small quartz tube under a nitrogen atmosphere inside a glove box. As in the previous step, this tube was placed inside a larger quartz synthesis tube, evacuated, and sealed. The mixture underwent a two-step heat treatment: first at 450 °C, followed by 650 °C, each for 24 hours to ensure complete reaction. The product was

doi:10.6342/NTU202503490

subsequently reground and analyzed by XRD to verify the formation of polycrystalline Fe_3GaTe_2.

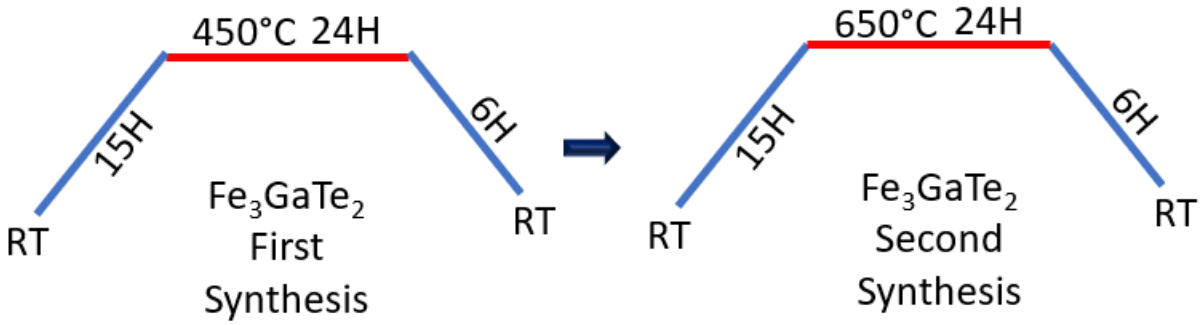

Figure 02.08: Temperature–time profile used in the two stages synthesis of Fe_3GaTe_2

To obtain single crystals, approximately 200 mg of iodine was added as a transport agent to the polycrystalline Fe_3GaTe_2 powder. The mixture was sealed in a quartz tube (41 cm in length, 22 mm in diameter) under vacuum, again within a nitrogen-filled glove box. This tube was placed in a two-zone horizontal tube furnace, with the source zone maintained at 750 °C and the growth zone at 700 °C. The CVT process proceeded over 200 hours, during which the temperature gradient facilitated the transport of Fe_3GaTe_2 vapors and the deposition of single crystals in the cooler region. The resulting crystals, measuring up to several millimeters in size, were confirmed by XRD analysis. This CVT-based approach, utilizing iodine as a transport agent, is a widely recognized method for growing high-quality single crystals of layered chalcogenides [75-77].

doi:10.6342/NTU202503490

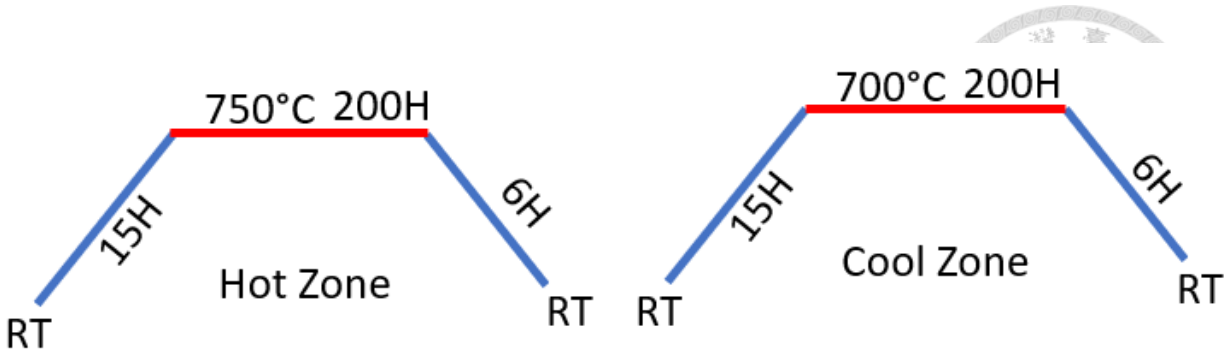

Figure 02.09: Temperature–time profile used in the single crystal growth of Fe_3GaTe_2

2.3. Structural and Compositional Characterization

2.3.1 Optical Microscopy Images

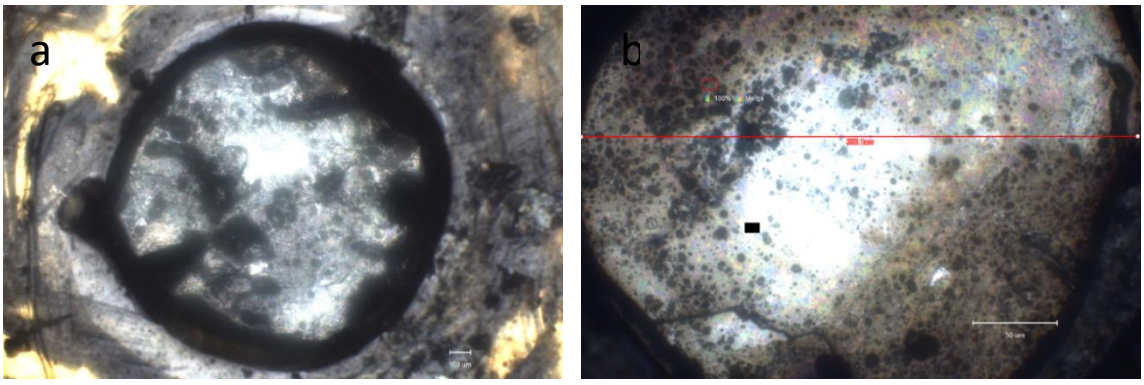

Figure 02.10: Optical Microscope image of surface of (a) Fe_3GeTe_2 (b) Fe_3GaTe_2

The optical microscopy images were taken at MY Lab (Room Number; 218), IAMS, Academia Sinica, Taipei, Taiwan.

As an initial step to examine the morphology of the synthesized crystals, optical microscopy was employed prior to scanning electron microscopy (SEM). The optical images of Fe_3GeTe_2 (FGT) and Fe_3GaTe_2 (FGaT) are presented in Figure 02.10. These images provide a macroscopic view of the surface and allow for a preliminary assessment of the overall crystal quality. While optical microscopy does not provide sufficient resolution to analyze fine

doi:10.6342/NTU202503490

structural details, it serves as an essential first step in identifying macroscopic uniformity and surface quality.

2.3.2 Energy Dispersive X-ray Spectroscopy (EDS) and Elemental Analysis

EDS was taken at Instrumentation Center, National Taiwan University, Taipei, Taiwan (Hitachi SU8220).

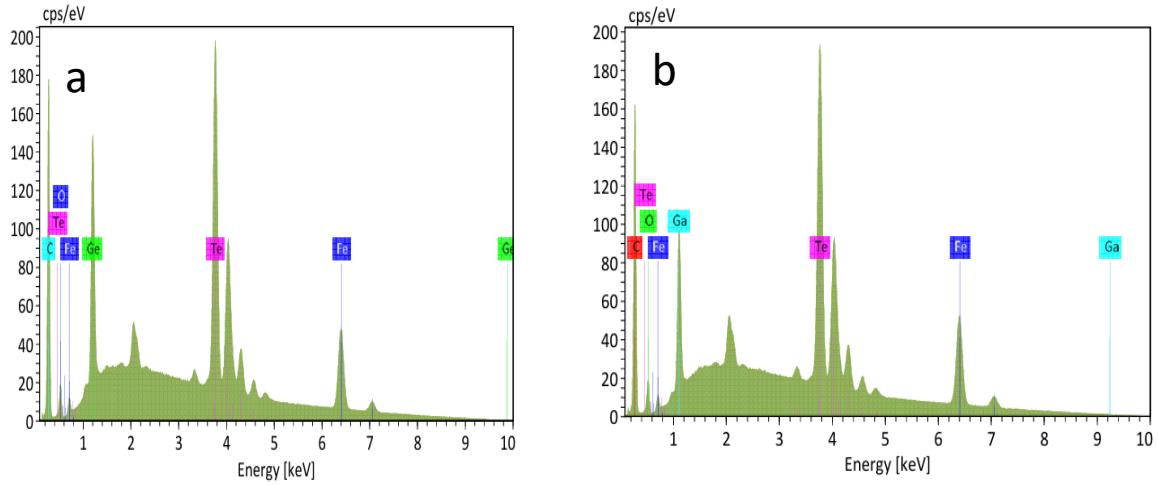

Figure 02.11: EDS spectra (a) Fe_3GeTe_2 (b) Fe_3GaTe_2

Acquisition 71

Element	At. No.	Line s.	Mass Norm. [%]	Atom [%]
Iron	26	K-Serie	38.75	55.46
Gallium	31	L-Serie	11.85	13.59
Tellurium	52	L-Serie	49.40	30.95
			100.00	**100.00**

Acquisition 72

Element	At. No.	Line s.	Mass Norm. [%]	Atom [%]
Iron	26	K-Serie	35.53	51.55
Germanium	32	L-Serie	15.62	17.43
Tellurium	52	L-Serie	48.84	31.01
			100.00	**100.00**

Energy-dispersive X-ray spectroscopy (EDX) was employed to determine the elemental composition of the synthesized Fe_3GaTe_2 and Fe_3GeTe_2 single crystals. This technique operates by detecting characteristic X-rays emitted when a focused electron beam interacts

doi:10.6342/NTU202503490

with a material inside a scanning electron microscope (SEM). Since each element produces X-rays at distinct energies, the method enables both qualitative identification and quantitative assessment of the constituent elements. Owing to its precision, EDX has become indispensable in verifying stoichiometry, identifying possible impurities, and confirming the compositional uniformity of newly synthesized materials.

In the present study, the EDX spectra of Fe_3GaTe_2 and Fe_3GeTe_2 revealed pronounced peaks corresponding to iron (Fe), tellurium (Te), and either gallium (Ga) or germanium (Ge), without any signals from extraneous elements. This absence of impurity peaks strongly indicates that the crystals possess high chemical purity. Quantitative analysis further demonstrated that the measured atomic percentages closely match the nominal stoichiometry of the compounds. For Fe_3GaTe_2, the composition was determined to be Fe: 55.46%, Ga: 13.59%, and Te: 30.95%, while Fe_3GeTe_2 exhibited Fe: 51.55%, Ge: 17.43%, and Te: 31.01%. These results correspond well to the expected 3:1:2 ratio for Fe:Ga/Ge:Te, thereby confirming the successful synthesis of both materials.

The measured values are also consistent with those previously reported in the literature. The Fe_3GaTe_2 matches with the data reported by [78] and Fe_3GeTe_2 are in excellent agreement with [79], Such consistency not only validates the reliability of our synthesis method but also reinforces the accuracy of EDX as a characterization technique for layered tellurides. Overall, the results confirm that both Fe_3GaTe_2 and Fe_3GeTe_2 were synthesized with the desired stoichiometry and purity, establishing a robust basis for further structural and electrochemical investigations.

doi:10.6342/NTU202503490

2.3.3 X-ray Diffraction (XRD) Analysis

XRD was taken at NMCGL (Dr. Raman Sankar Lab) at Institute of Physics, Academia Sinica, Taipei, Tiwan (Bruker D2 PHASER).

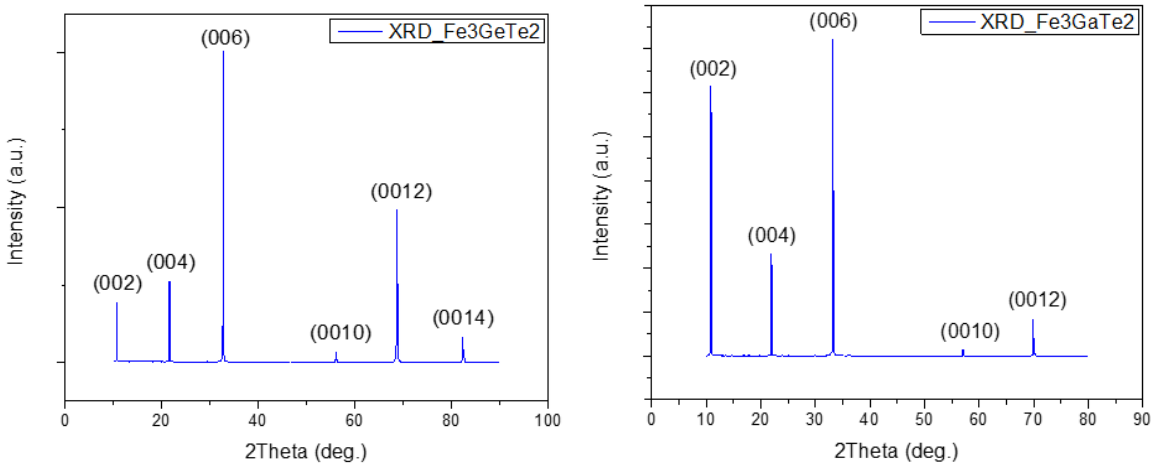

Figure 02.12: XRD patterns of (a) Fe_3GeTe_2 (b) Fe_3GaTe_2

X-ray diffraction (XRD) is a widely used technique for probing the crystallographic structure, phase purity, and orientation of crystalline materials. When X-rays interact with the periodic arrangement of atoms in a crystal, they are diffracted according to Bragg's law ($2d\sin\theta = n\lambda$). Analysis of the diffraction pattern provides direct information on lattice parameters, the identity of crystallographic planes, and the degree of crystallinity. For layered and two-dimensional materials, XRD is particularly effective in verifying preferred orientation along the c-axis and identifying the absence or presence of secondary phases. Such information is crucial for assessing the structural quality of single crystals like Fe_3GaTe_2 (FGaT) and Fe_3GeTe_2 (FGT), which are the focus of this study.

doi:10.6342/NTU202503490

The XRD patterns obtained for both FGT and FGaT reveal only (00l) reflections, including (002), (004), (006), (0010), and (0012), which confirms that both materials exhibit a pronounced c-axis orientation and retain their layered single-crystal nature. The absence of non-(00l) peaks indicates high phase purity and the lack of contributions from randomly oriented crystallites, demonstrating that the synthesized samples are of excellent quality.

To validate the accuracy of these results, the XRD pattern of Fe_3GaTe_2 was compared with previously reported data [80] and of Fe_3GeTe_2 with [81]. The perfect match in both peak positions and relative intensities confirms the reliability of our synthesis and characterization process.

In addition to phase identification, the diffraction results provide important insight into lattice parameters. For FGT, the extracted c-axis parameter was found to be approximately 1.633 nm, For FGaT, the c-axis parameter was slightly smaller, approximately 1.623 nm. The small but systematic difference in lattice parameters explains the slight shift of diffraction peaks toward lower 2θ values in FGT compared to FGaT, as observed in the overlaid XRD patterns. This relationship arises directly from Bragg's law: a larger c-axis increases the interplanar spacing (d), which in turn shifts the diffraction peaks to smaller 2θ angles.

Taken together, these results confirm that Fe_3GaTe_2 and Fe_3GeTe_2 are isostructural, sharing the same layered hexagonal structure, but with subtle differences in lattice constants that can be directly correlated with elemental substitution. The consistency between experimental measurements and reference data further underscores the structural integrity of the synthesized crystals and validates their suitability for subsequent physical property and electrochemical investigations.

doi:10.6342/NTU202503490

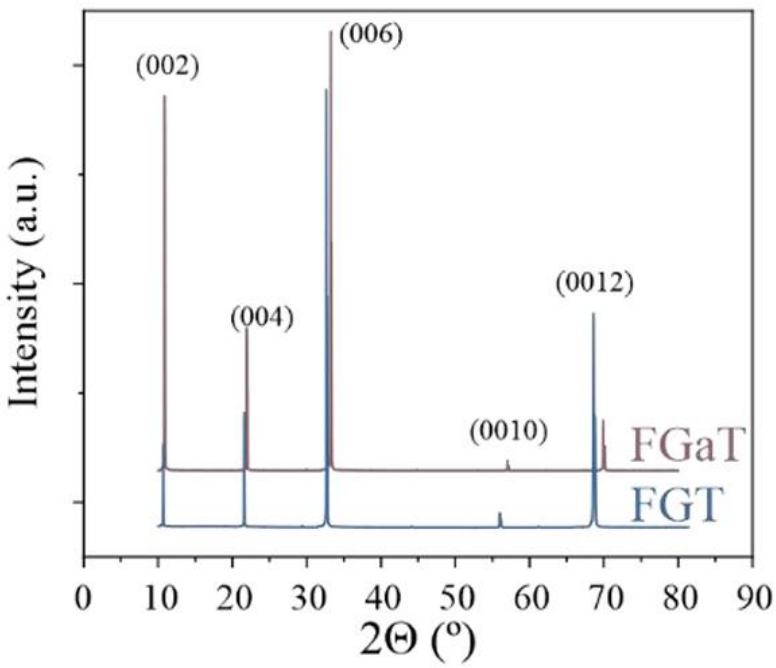

Figure 02.13: Joint XRD patterns of (a) Fe_3GeTe_2 (b) Fe_3GaTe_2

2.3.4 Scanning Electron Microscope

SEM image was taken at Instrumentation Center, National Taiwan University (Hitachi SU8220).

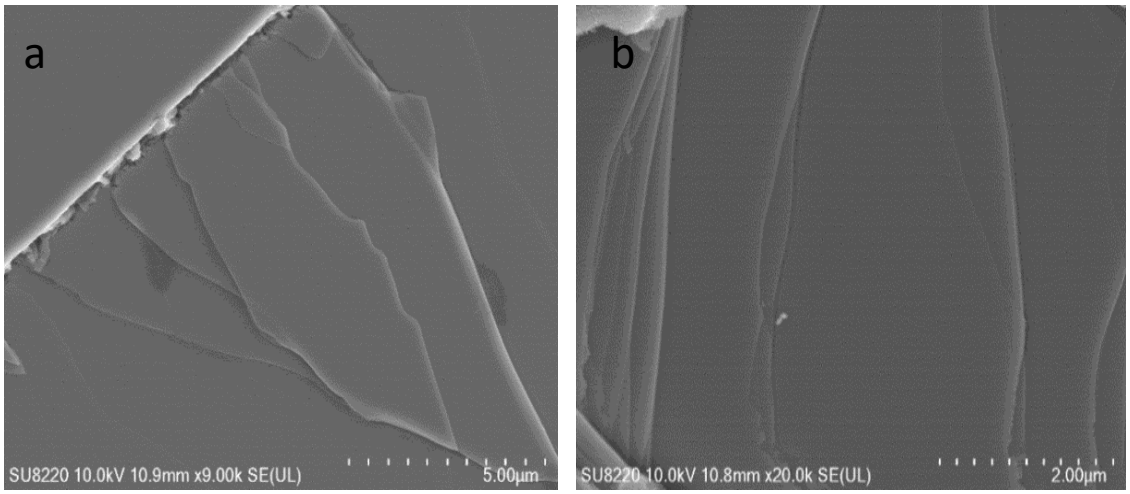

Figure 02.14: SEM image of surface of (a) Fe_3GeTe_2 (b) Fe_3GaTe_2

doi:10.6342/NTU202503490

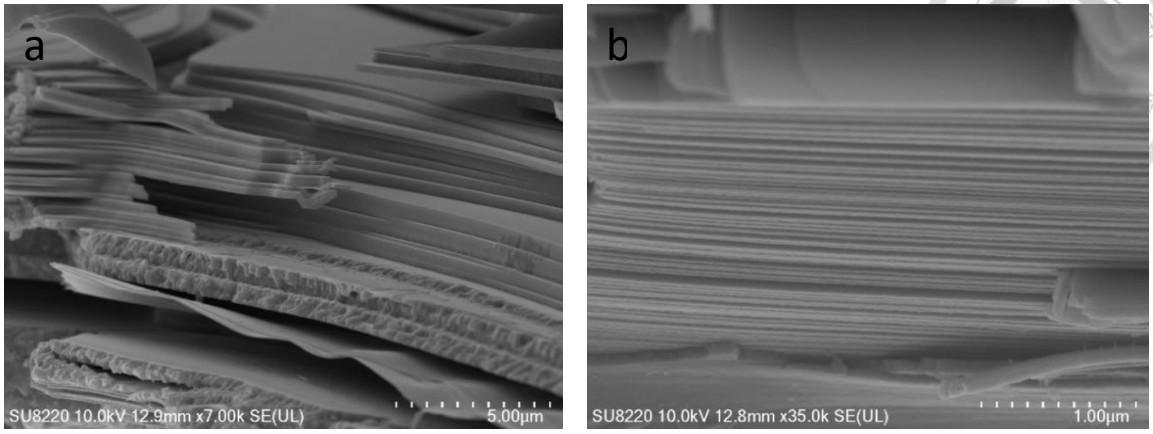

Figure 02.15: SEM image of Cross-section of (a) Fe_3GeTe_2 (b) Fe_3GaTe_2

Following the confirmation of crystal structure and phase purity by X-ray diffraction, scanning electron microscopy (SEM) was employed to further investigate the morphology of the Fe_3GaTe_2 (FGaT) and Fe_3GeTe_2 (FGT) single crystals. While XRD provides information on crystallographic orientation and lattice parameters, SEM enables direct visualization of surface features and internal stacking, offering complementary insight into the quality of the synthesized crystals.

The surface images of both compounds display the characteristic features of van der Waals layered materials, with large, flat terraces separated by distinct step edges. In the case of Fe_3GaTe_2, terraces observed at 20,000× magnification with a 2.00 μm scale bar are smooth and sharply defined, reflecting excellent crystallinity and a low density of structural imperfections. Fe_3GeTe_2 shows a comparable terraced morphology at 9,000× magnification with a 5.00 μm scale bar, though the terraces appear broader with slightly less well-defined edges. These observations provide strong visual confirmation of the layered nature of both compounds and reinforce the conclusions drawn from XRD regarding the high crystalline quality of the samples.

doi:10.6342/NTU202503490

Cross-sectional SEM images complement the surface observations by revealing the internal architecture of the crystals. Fe_3GaTe_2 exhibits a highly ordered stacking sequence at 35,000× magnification with a 1.00 μm scale bar, with parallel layers extending uniformly across the sample. By comparison, Fe_3GeTe_2, examined at 7,000× magnification with a 5.00 μm scale bar, also shows layered stacking but with minor irregularities such as folding and uneven edges. These features are likely linked to sample preparation during SEM mounting and cleaving, although slight intrinsic variations cannot be completely excluded.

Together with the XRD results, the SEM analysis provides a coherent picture of the structural and morphological integrity of the synthesized single crystals. The agreement between crystallographic confirmation and morphological visualization demonstrates the effectiveness of the growth process and establishes a strong foundation for subsequent Raman, electronic, and electrochemical characterizations.

2.3.5 Raman Spectroscopy & Optical Characterization

Raman Spectra was taken at MY Lab (Room Number; 218), IAMS, Academia Sinica.

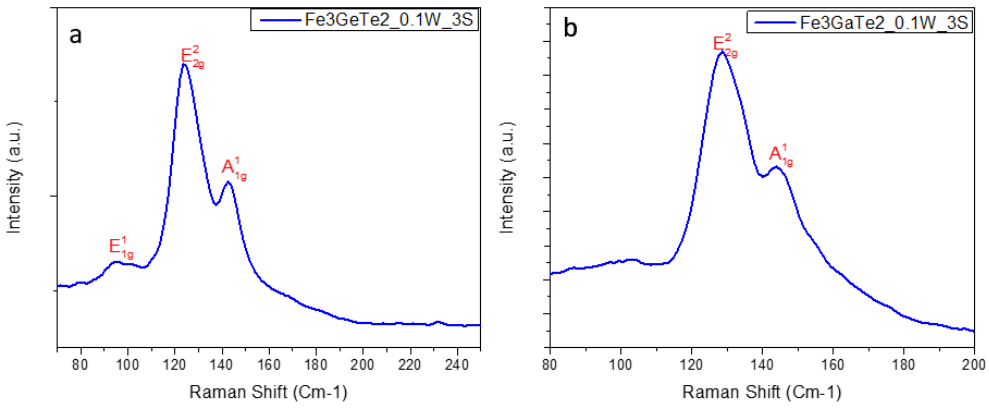

Figure 02.16: Raman Spectra of (a) Fe_3GeTe_2 (b) Fe_3GaTe_2

doi:10.6342/NTU202503490

Raman spectroscopy was employed to further investigate the vibrational properties and structural integrity of the Fe_3GaTe_2 (FGaT) and Fe_3GeTe_2 (FGT) single crystals. This technique provides critical insight into lattice dynamics, since the observed Raman-active modes are directly linked to the symmetry and bonding environment of the atoms within the crystal lattice. In layered transition metal tellurides, such as FGT and FGaT, the most prominent modes correspond to vibrations of the heavy tellurium atoms, as these dominate the Raman response due to their larger polarizability compared with the lighter Fe or Ga/Ge atoms.

The Raman spectrum of FGaT reveals two dominant peaks centered at approximately 126 cm^{-1} and 142 cm^{-1}. These are assigned to the E_{2g} and A_{1g} modes, respectively. The A_{1g} mode represents out-of-plane vibrations of Te atoms, where the atoms oscillate perpendicular to the basal plane of the layered structure. In contrast, the E_{2g} mode corresponds to in-plane vibrations, where the Te atoms move parallel to the basal plane in a coordinated pattern. These assignments are consistent with the expected vibrational behavior of van der Waals-layered materials and reflect the high crystallographic order of the synthesized FGaT.

For FGT, the Raman spectrum exhibits three distinguishable peaks. At lower wavenumbers, a weak E_{1g} mode is detected, followed by the E_{2g} mode near 130 cm^{-1} and the A_{1g} mode around 150 cm^{-1}. As in FGaT, the E-type modes represent in-plane vibrations, while the A_{1g} mode corresponds to out-of-plane motion. The appearance of the E_{1g} mode in FGT, absent in FGaT, is consistent with subtle differences in lattice symmetry and vibrational coupling introduced by the substitution of Ge for Ga.

doi:10.6342/NTU202503490

A comparison between the two spectra reveals that the peaks of FGaT occur at slightly higher wavenumbers than those of FGT. A shift to higher Raman frequencies indicates stiffer vibrational force constants and stronger bonding interactions. This effect can be rationalized by considering that Ga substitution alters the local bonding environment of Te, leading to enhanced bond stiffness and thus higher-energy phonon modes. These results validate the impact of elemental substitution on lattice dynamics and highlight how subtle structural changes influence vibrational properties.

The accuracy of these Raman assignments was confirmed through direct comparison with published literature. The Raman spectrum of FGaT matches closely with earlier reports [82] , showing nearly identical peak positions and relative intensities, while the vibrational features of FGT are consistent with those reported in [83]. This close correspondence provides strong validation for the reliability of our synthesis and confirms the correct identification of the vibrational fingerprints of both materials.

From a broader perspective, the identification of in-plane (E_{2g}) and out-of-plane (A_{1g}) modes is of particular importance for layered materials. In-plane vibrations are closely related to basal-plane bonding interactions, while out-of-plane vibrations provide insight into interlayer coupling across the van der Waals gaps. Therefore, Raman spectroscopy not only confirms the structural integrity of our synthesized crystals but also provides direct evidence of the changes in interatomic interactions induced by Ga substitution. Taken together, the Raman results demonstrate that while both FGT and FGaT preserve the expected layered vibrational behavior, the subtle shift in wavenumbers reflects meaningful differences in bonding stiffness that may ultimately influence the electrochemical stability of these materials.

doi:10.6342/NTU202503490

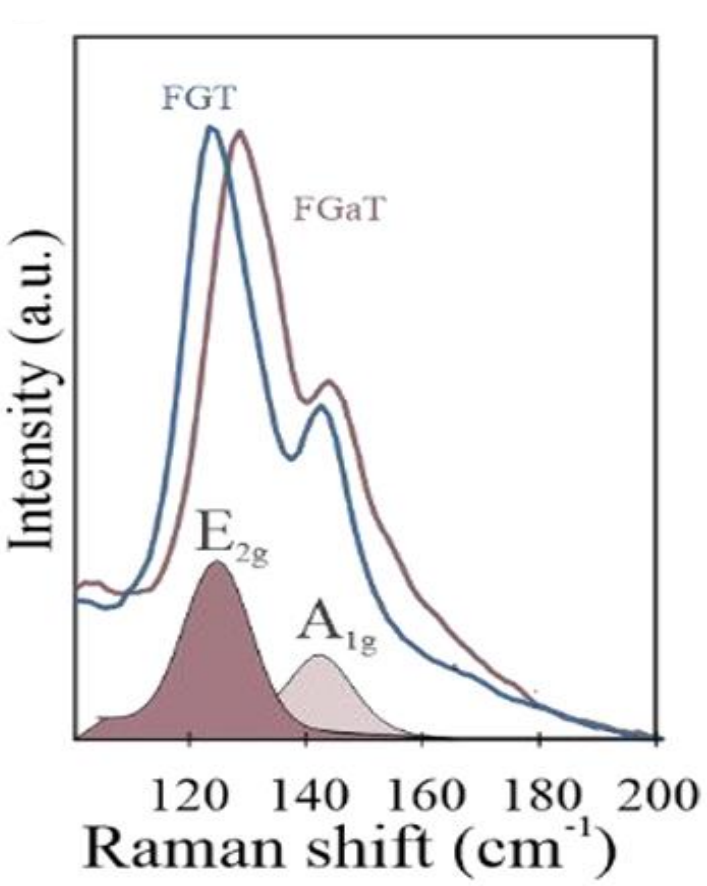

Figure 02.17: Joint Raman spectra of FGT and FGaT with deconvolution of FGT into E_{2g} and A_{1g} modes

2.4. Conclusion

The present study demonstrates that the Chemical Vapor Transport (CVT) method is a highly effective route for synthesizing high-quality single crystals of Fe_3GaTe_2 and Fe_3GeTe_2. By carefully optimizing growth parameters such as the concentration of the transport agent and the applied temperature gradient, it was possible to produce crystals with superior crystallinity, larger dimensions, and fewer structural defects compared to those reported in earlier studies. The success of this optimization highlights the importance of fine-tuning experimental conditions to achieve reproducible and well-ordered growth in van der Waals layered compounds.

doi:10.6342/NTU202503490

A particularly significant outcome of this work is the ability to grow Fe_3GaTe_2 crystals with lateral dimensions of up to 3 mm, which represents a clear improvement over prior reports that typically described much smaller crystal sizes. Alongside the improvement in size, the crystals obtained in this study were confirmed to possess high phase purity through complementary characterization techniques. X-ray diffraction (XRD) confirmed the absence of secondary phases and verified the strong crystallographic orientation of the samples, while energy-dispersive X-ray spectroscopy (EDS) validated the stoichiometric composition. These findings ensure that the physical and chemical properties investigated in subsequent sections reflect the intrinsic behavior of Fe_3GaTe_2 and Fe_3GeTe_2, without interference from impurities or extraneous phases.

In addition to establishing the effectiveness of the CVT method, the study also provided new insights into the growth dynamics of these materials. It was observed that variations in the concentration of the transport agent exert a measurable influence on both nucleation density and the resulting crystal morphology. These observations not only clarify the mechanisms underlying CVT-based crystal growth but also contribute to the broader understanding of how to systematically control the growth of two-dimensional layered crystals.

Taken together, these results underscore the CVT technique as a robust and versatile method for producing high-quality crystals of Fe_3GaTe_2 and Fe_3GeTe_2. The improved crystal size, enhanced phase purity, and deeper understanding of the growth process provide a strong foundation for future research. Importantly, the high-quality crystals obtained in this study are well suited for advanced physical investigations, including studies in spintronics and

doi:10.6342/NTU202503490

topological physics, where material quality plays a decisive role in uncovering intrinsic quantum phenomena.

doi:10.6342/NTU202503490

doi:10.6342/NTU202503490

CHAPTER: 03

ELECTROCHEMISTRY ON Fe_3GaTe_2 AND Fe_3GeTe_2

3.1 Electrochemical Characterization: Methodological Considerations and Rationale

Having confirmed the structural and compositional similarity of the synthesized materials through comprehensive characterization techniques, the subsequent step in this study involves a detailed investigation of their electrochemical behavior. Understanding the intrinsic electrochemical properties is critical for evaluating their potential applications, particularly in catalysis and energy conversion systems.

Traditional electrochemical characterization methods, as widely reported in the literature, often involve the use of exfoliated or powdered samples that are dispersed onto conductive substrates such as glassy carbon electrodes or metal foils for catalytic activity assessment [83, 84]. One significant drawback of these conventional configurations is their inability to distinguish between the catalytic contributions arising from the basal planes of the material and those originating from edges or defect sites. This distinction is crucial because the catalytic activity is not uniformly distributed across the material's surface. Edge sites and defects typically exhibit enhanced reactivity due to their unsaturated coordination environment and modified electronic structures, which differ markedly from the more inert basal planes [85]. Consequently, the overall catalytic performance observed in such studies is often dominated by these edge effects, potentially obscuring the intrinsic properties of the basal planes themselves.

doi:10.6342/NTU202503490

This phenomenon has been extensively documented in transition metal dichalcogenides and related layered materials, where the edge sites serve as active centers for various electrochemical reactions, including hydrogen evolution and oxygen reduction [86, 87]. The altered electronic states at these edges facilitate enhanced adsorption and activation of reactant molecules, thereby significantly influencing the measured catalytic activity.

Given these considerations, the present study adopts a novel electrochemical characterization approach designed to more accurately probe the intrinsic activity of the basal planes, minimizing the confounding effects of edges and defects. This methodological refinement is essential for developing a fundamental understanding of the material's catalytic mechanisms and guiding the rational design of improved electrocatalysts.

3.2 Experimental Strategy to Isolate Basal Plane Activity

To address the inherent challenges associated with differentiating the electrochemical activity of basal planes from that of edges and defect sites, we developed a strategic experimental approach that leverages the unique physical characteristics of our synthesized single crystals. Specifically, the large lateral dimensions of these crystals provide a significant advantage, enabling us to selectively expose the basal plane while effectively minimizing the influence of edge-related phenomena.

To implement this design, we fabricated a custom silicone membrane tailored precisely to encapsulate the single crystal sample. The membrane serves multiple essential functions. First, it physically isolates the edges of the crystal by covering and sealing them, thereby preventing any direct contact between these regions and the electrolyte. This selective

doi:10.6342/NTU202503490

exposure ensures that the electrochemical reactions occur predominantly at the basal plane. Second, the membrane is engineered to prevent the electrolyte from reaching the underlying conductive substrate, which is commonly used to support the sample. This is a critical consideration because any direct electrolyte-substrate interaction could introduce additional electrochemical signals unrelated to the material under study, thereby confounding the interpretation of results.

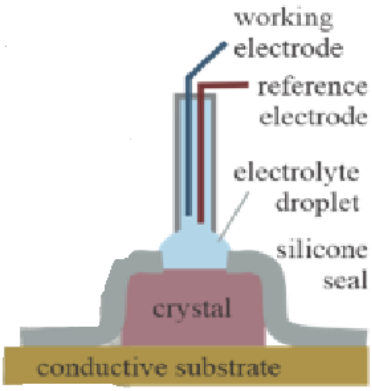

Figure 03.01: Schematic of the electrochemical device configuration with a silicone membrane used to isolate the basal plane of the single crystal from the edges and substrate

Moreover, the use of a silicone membrane offers practical advantages, including chemical inertness, flexibility, and ease of fabrication, making it an ideal choice for such selective encapsulation. This approach can be adapted and extended to other layered materials and electrochemical systems where distinguishing between different surface sites is crucial.

3.3 Electrode Preparation

To prepare the electrode, a standard glass slide was selected as the substrate. A thin layer of gold was deposited onto the glass surface using the **Physical Vapor Deposition (PVD)**

doi:10.6342/NTU202503490

technique. This gold coating was necessary to render the surface conductive. Following the deposition, silver paint was carefully applied to define the electrode region.

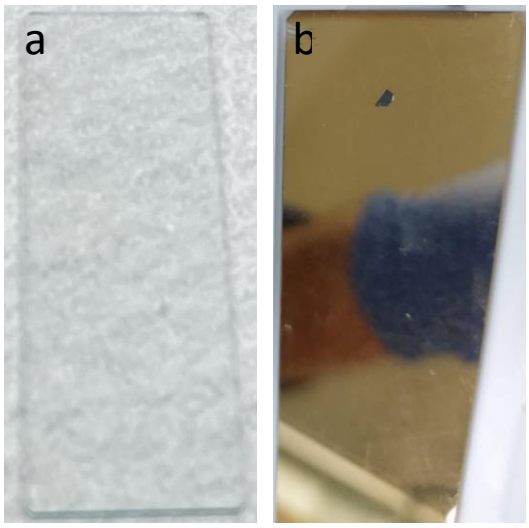

Figure 3.2: (a) Bare glass substrate used as the base for electrode fabrication. (b) Glass slide after gold (Au) layer deposition, forming a conductive surface. A crystal of FGT or FGaT is attached to the gold surface using silver paint, which acts as a conductive adhesive layer to ensure good electrical contact between the crystal and the gold electrode

Next, the catalyst materials under investigation, **Fe_3GeTe_2 and Fe_3GaTe_2**, were deposited onto one of the electrodes. The catalyst materials were then left to dry naturally at room temperature for a minimum duration of **24 hours** to ensure proper adhesion and stability.

In order to confine the electrolyte exclusively to the catalyst area, a **silicone mask** was prepared. A precise circular hole, slightly smaller than the sample size, was cut at the center of the silicon sheet. The silicone mask is having with a **plastic adhesive layer**. To position it correctly on the sample, the protective plastic layer was carefully removed, allowing the adhesive-coated silicon sheet to be affixed onto the gold-coated glass slide. This

doi:10.6342/NTU202503490

configuration ensured that the small circular opening in the silicon sheet was perfectly aligned with the catalyst material.

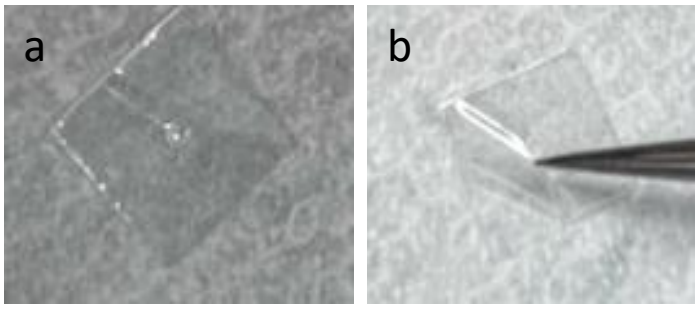

Figure 03.03: (a) Silicone Mask with circular hole at the center (b) Adhesive Plastic Layer

After securing the silicone mask, the **electrolyte solution** was introduced into the confined region, ensuring that it completely covered the catalyst material. A crucial aspect of this step was **to prevent any direct contact between the electrolyte and the gold-coated surface.** Any unintentional electrolyte-gold interaction would result in direct electrical conductivity, thereby compromising the experiment by allowing an unwanted electrical pathway. Therefore, extreme caution was exercised to **maintain accuracy and precision** throughout the preparation process.

3.4 Electrochemical Measurement Setup

The electrochemical measurement setup for evaluating the hydrogen evolution reaction (HER) performance of Fe_3GaTe_2 and Fe_3GeTe_2 involves a three-electrode system configuration. This setup is widely used in electrochemical experiments due to its ability to control and measure the potential of the working electrode independently of the counter electrode.

doi:10.6342/NTU202503490

Three-Electrode System Configuration

1. **Working Electrode (Fe_3GaTe_2 and Fe_3GeTe_2):** The working electrodes are the materials under investigation, in this case, Fe_3GaTe_2 and Fe_3GeTe_2. These materials are prepared and mounted in a manner that ensures good electrical contact and exposure to the electrolyte. Self-supporting electrodes can be used directly, or they can be deposited onto a substrate like metal or glassy carbon.
2. **Counter Electrode (Platinum (Pt) Wire):** The counter electrode, typically made of a highly conductive and inert material like platinum (Pt), serves to complete the electrochemical circuit by facilitating a complementary reaction to that occurring at the working electrode. Pt is chosen for its high electrical conductivity and stability, ensuring that the counter electrode reaction does not limit the current flow during the experiment [88, 89].
3. **Reference Electrode** (**Ag/AgCl):** The reference electrode provides a stable potential against which the working electrode potential is measured.

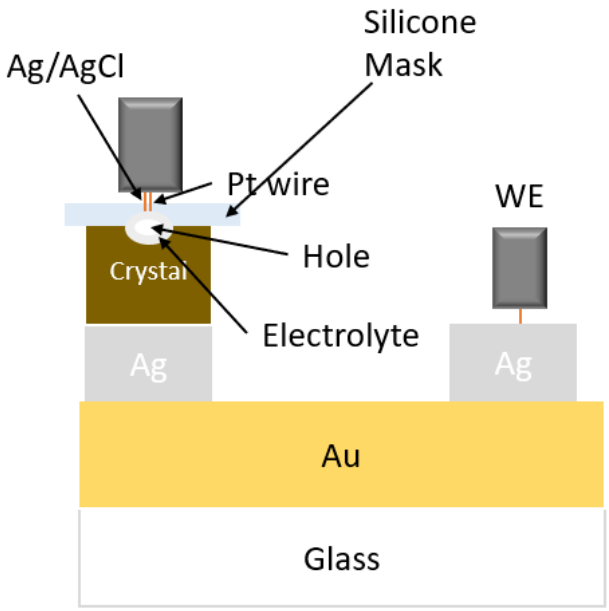

doi:10.6342/NTU202503490

Figure 03.04: Schematic illustration of the three-electrode microelectrochemical setup used for surface-limited electrochemical measurements. The system includes a layered crystal (FGT or FGaT) placed over a patterned Au contact on glass, with a silicone mask defining the electrolyte contact area through a central hole

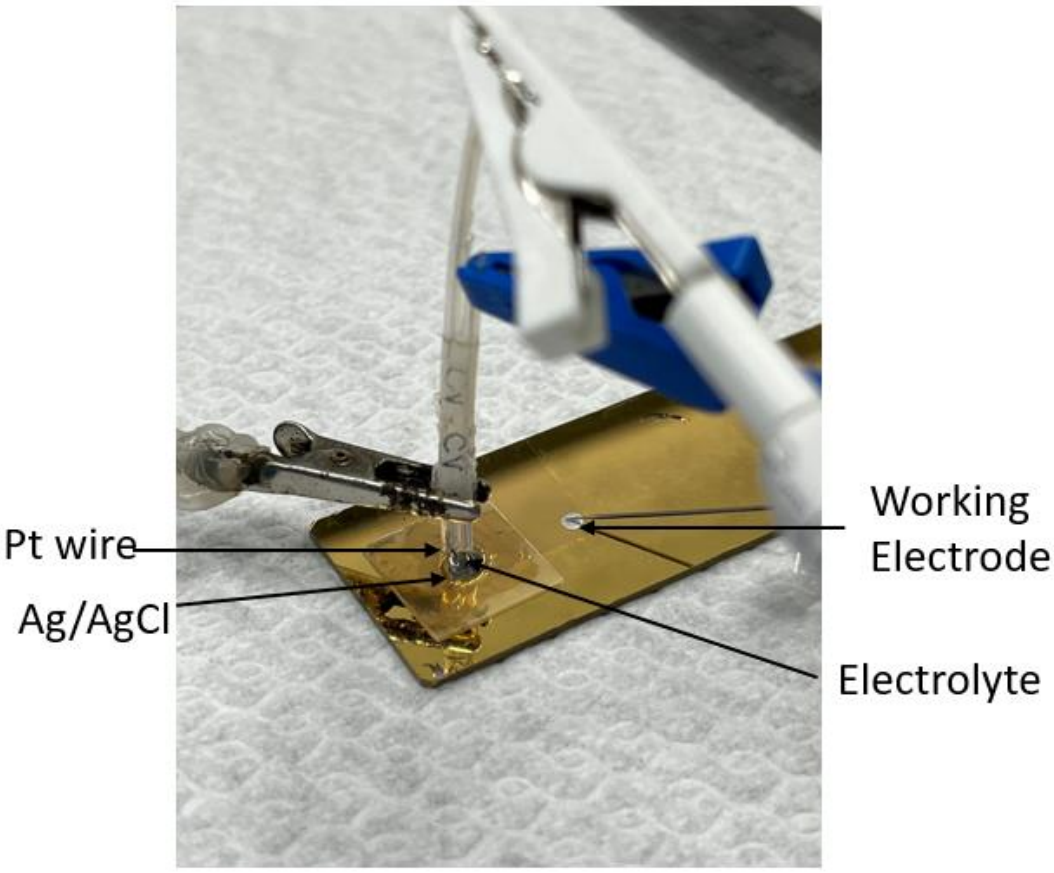

Figure 03.05: Three-electrode electrochemical setup used for LSV and Cyclic Voltammetry measurements. The configuration includes a Pt wire counter electrode, an Ag/AgCl reference electrode, and a working electrode (FGT or FGaT) immersed in electrolyte

doi:10.6342/NTU202503490

Instrumentation Used For electrochemical measurements, a potentiostat/galvanostat is essential for controlling the potential and current during experiments. Several manufacturers offer high-performance instrument. We have used SP-200 made by BioLogic.

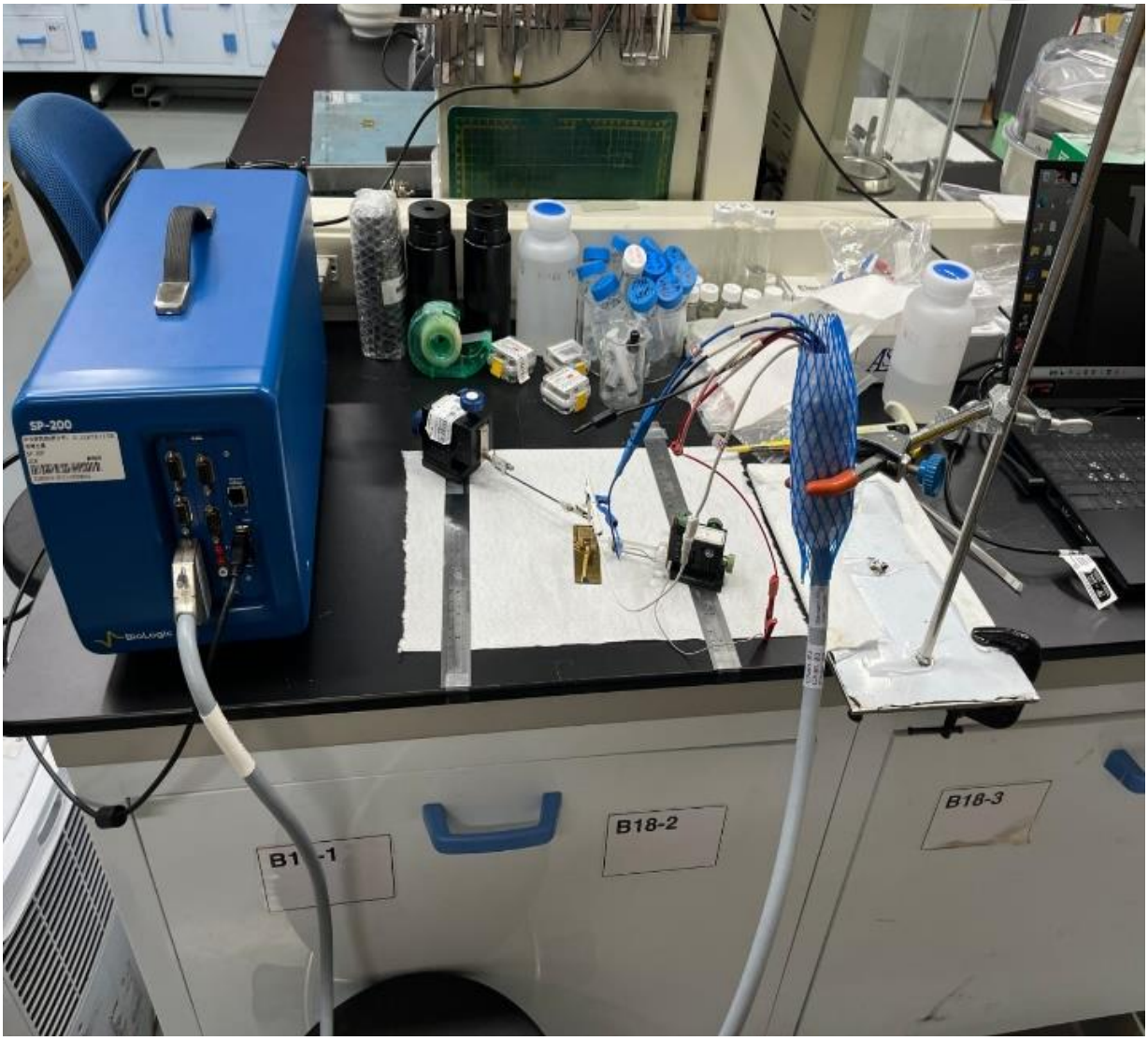

Figure 03.06: Electrochemical measurement setup using BioLogic SP-200 potentiostat/galvanostat. The system is configured for device testing, with electrical connections established for in situ measurements. Various lab accessories and components, including sample holders, electrolyte containers, and connecting electrodes, are arranged for precise control and monitoring during electrochemical experiments

doi:10.6342/NTU202503490

3.5 Electrochemical Performance and Basal Plane Activity

With the precisely controlled experimental setup designed to isolate basal plane contributions, we proceeded to evaluate the electrochemical performance of our synthesized materials, namely FGT and FGaT. Linear Sweep Voltammetry (LSV) was employed as the primary electrochemical technique to examine their catalytic activity, particularly towards the hydrogen evolution reaction (HER), within a 0.5 M H_2SO_4 solution. This electrolyte concentration ensures a sufficiently conductive medium and provides the necessary proton source for the HER.

3.5.1 Linear Sweep Voltammetry (LSV)

Linear Sweep Voltammetry (LSV) is a fundamental electrochemical technique extensively employed to investigate the redox properties, electrocatalytic activity, and charge transfer kinetics of materials at the working electrode interface [90, 91]. Unlike cyclic voltammetry, where the potential is swept forward and then reversed, LSV involves a unidirectional linear potential sweep at a constant scan rate, typically from a starting potential to a more positive or negative limit depending on the reaction of interest. This controlled potential ramp induces faradaic processes at specific potentials, generating a current response that is recorded as a voltammogram. The onset potential observed in the LSV curve marks the threshold at which the electrochemical reaction becomes thermodynamically and kinetically favorable, serving as a critical parameter to evaluate catalytic efficiency, particularly in reactions such as the hydrogen evolution reaction (HER), oxygen evolution reaction (OER), and fuel oxidation [92].

doi:10.6342/NTU202503490

A typical LSV profile features an initial capacitive (non-faradaic) current region followed by a sharp increase in current corresponding to the onset of the electrochemical reaction. The magnitude and slope of this increase provide insight into the catalyst's active surface area and intrinsic activity.

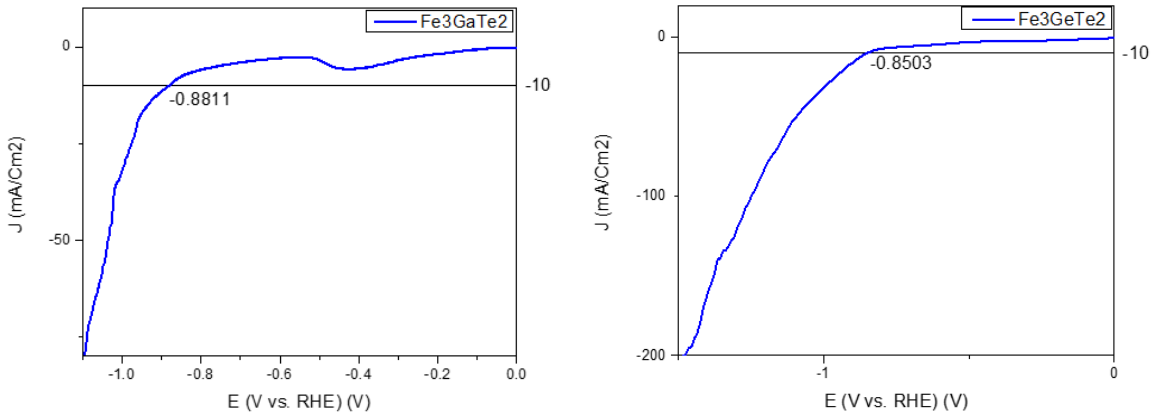

Figure 03.07: Linear sweep voltammetry (LSV) curves of Fe_3GaTe_2 (FGaT) and Fe_3GeTe_2 (FGT) recorded in 0.5 M H_2SO_4. The overpotentials required to achieve a current density of −10 mA/cm² are 0.88 V for FGaT (a) and 0.85 V for FGT (b)

3.5.2 Initial Observations and Disparity with Previous Studies

The LSV measurements revealed distinct catalytic behaviors when focusing solely on the basal planes. For FGT, the measured overpotential required to drive the HER was found to be approximately 0.85 V (as depicted in Figure 03.08). This value, obtained under strictly basal-plane-isolated conditions, stands in stark contrast to the significantly lower overpotentials typically reported in prior literature for similar materials [93].

doi:10.6342/NTU202503490

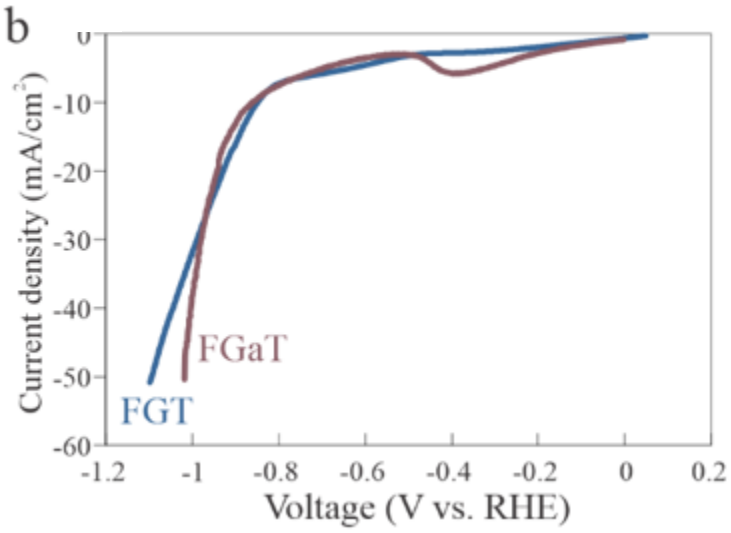

Figure 03.08: Linear sweep voltammetry (LSV) curves in 0.5 M H_2SO_4, showing similar overpotentials for FGT and FGaT

This substantial disparity unequivocally highlights the critical and often dominant role that edge sites and defects played in earlier electrochemical experiments that utilized exfoliated samples or powders. In those conventional configurations, the higher reactivity of edges and defect sites, stemming from their unsaturated coordination and altered electronic structures, invariably contributes a disproportionately large portion of the observed catalytic current. Consequently, the reported lower overpotentials in those studies were largely a reflection of the cumulative activity from these highly active sites rather than the intrinsic activity of the extended basal planes. Our current findings, by effectively negating edge contributions, therefore provide a more accurate representation of the fundamental, lower catalytic activity inherent to the pristine basal surfaces of FGT. This underscores the importance of our refined experimental methodology in deciphering the true intrinsic activity of different material facets.

doi:10.6342/NTU202503490

3.5.3 Comparative Basal Plane Activity of FGT and FGaT

Importantly, when comparing the two materials under investigation, FGaT exhibited a remarkably similar overpotential of approximately 0.88 V for the HER. The close proximity of these overpotential values for FGT and FGaT strongly suggests that the intrinsic basal-plane activity of both materials is quantitatively comparable. This observation provides crucial evidence that the strategic gallium doping, while potentially influencing other material properties or edge activity, does not fundamentally alter the inherent catalytic inertness or activity of the basal planes themselves. This indicates that the primary catalytic active sites, if any, on the basal plane are not significantly modified by the introduction of gallium, at least under these specific electrochemical conditions.

3.5.4 Impact of Conductivity and Tafel Analysis

Additionally, the Tafel slope, derived from the logarithmic plot of current density versus overpotential, reveals mechanistic details and the rate-determining step of the reaction, enabling comparative analysis across different electrocatalysts [90].

Upon closer inspection of the LSV curves, a slightly steeper slope was observed for FGaT (Inset Figure 03.09). This difference was carefully investigated and attributed to the enhanced electrical conductivity of FGaT compared to FGT. Improved conductivity in electrocatalytic systems leads to a reduction in uncompensated resistance, as current can flow more freely through the material to the reaction interface [90]. Lower uncompensated resistance manifests as a steeper slope in the LSV or Tafel plot, which can initially obscure the true kinetic differences between materials.

doi:10.6342/NTU202503490

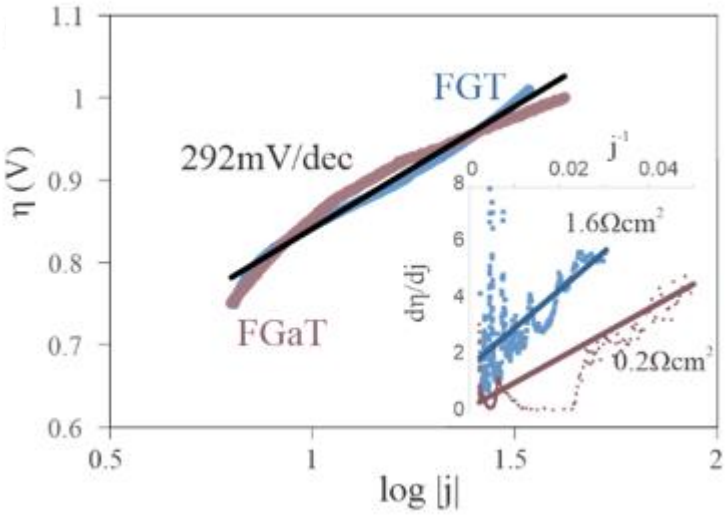

Figure 03.09: Tafel analysis confirming that both materials exhibit comparable intrinsic HER kinetics, (inset) graphical characterization of uncompensated resistance according to[93].

To account for this effect and enable a direct comparison of the intrinsic reaction kinetics, a resistance correction was applied to the raw LSV data for both materials. This correction removes the ohmic potential drop (iR drop) from the measured overpotential, allowing for a clearer depiction of the actual overpotential required to drive the reaction. Following this crucial resistance correction, the Tafel plots for both FGT and FGaT converged onto the same linear trend (Figure 03.09). The remarkable convergence of their Tafel slopes after correction quantitatively confirms the profound similarity of their intrinsic hydrogen evolution kinetics on the basal plane. This implies that the fundamental reaction mechanism and the rate-determining step for HER on the basal surfaces of both materials are essentially identical. The agreement in Tafel slopes, a direct measure of reaction kinetics, further reinforces the

doi:10.6342/NTU202503490

conclusion that gallium doping does not introduce new or significantly more active sites on the basal plane for HER.

This detailed analysis not only confirms the successful isolation of basal plane activity but also provides a more nuanced understanding of the inherent catalytic limitations of these specific facets. It also sets the stage for future investigations into how deliberate structural modifications or defect engineering could potentially activate these otherwise relatively inert basal planes.

3.5.6 Mechanistic Insights into Basal Plane Catalytic Activity

The observed similarity in the intrinsic catalytic activity of the basal planes of FGT and FGaT can be rationalized by examining the fundamental catalytic mechanism at the atomic level. Previous investigations into layered transition metal chalcogenides have identified that the primary active sites for hydrogen adsorption during the hydrogen evolution reaction (HER) are associated with specific top-site geometries on the chalcogen-terminated surfaces [94]. These top sites correspond to the positions directly above chalcogen atoms, where hydrogen adsorption is energetically favorable.

Importantly, these active sites are characterized by their limited electronic and structural interaction with the underlying metal sublayer atoms, such as Ga or Ge in our materials. This weak coupling implies that substitution of the sublayer element, replacing Ge with Ga, does not substantially alter the local electronic environment of the chalcogen surface atoms responsible for catalysis. Consequently, the catalytic performance of the basal plane remains largely unaffected by this compositional variation.

doi:10.6342/NTU202503490

To rigorously test this hypothesis and gain deeper insight into the electronic factors governing catalytic activity, we performed density functional theory (DFT) calculations focused on the electronic structure of both FGT and FGaT. Using projected density of states (PDOS) analysis, we examined the contributions of different atomic orbitals near the Fermi level, which is critical as the electronic states at or near the Fermi energy predominantly determine the material's chemical reactivity and catalytic behavior [95, 96].

The PDOS results, illustrated in Figure 03.10, reveal that the density of states near the Fermi level is overwhelmingly dominated by the Fe d-orbitals in both materials. This finding indicates that the Fe atoms, rather than the sublayer Ga or Ge atoms, play the principal role in governing the electrochemical properties and catalytic activity of the basal plane. The minimal contribution of Ga or Ge states near the Fermi level supports the experimental observation that substitution of these elements does not significantly impact the intrinsic catalytic behavior.

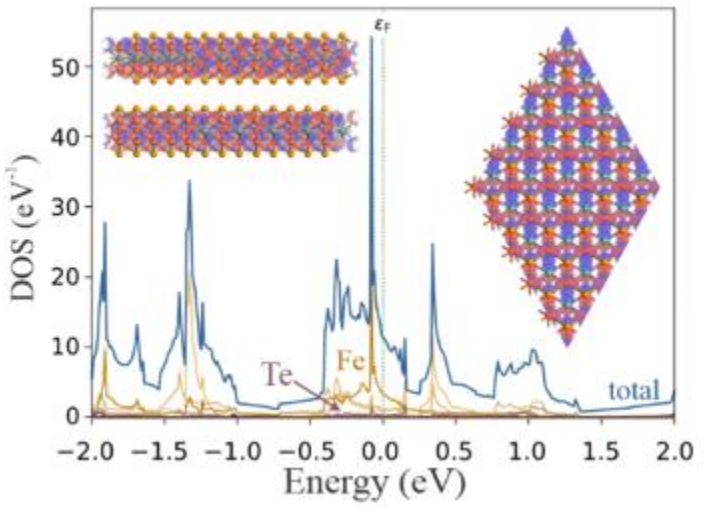

doi:10.6342/NTU202503490

Figure 03.10: FGT Density of states (DOS) projected onto Fe, Ge and Te atoms from DFT calculations, (inset) Structural model of eigenstate near the Fermi level decomposed into orbital contributions around Fe (red), Te (orange), and Ge (green) atoms confirming dominance of Fe and Te orbitals and minimal contribution of Ge atoms

This electronic structure analysis aligns well with the experimental electrochemical data, providing a coherent picture that the basal-plane catalytic activity is primarily controlled by the Fe centers. The chalcogen atoms provide the surface sites for hydrogen adsorption, while the underlying Fe d-orbitals facilitate electron transfer processes essential for the HER. The substitution of sublayer atoms, therefore, modulates bulk properties such as conductivity or stability but does not fundamentally alter the catalytic mechanism at the basal surface.

These insights are consistent with broader theoretical and experimental studies on transition metal dichalcogenides and related layered materials, where the transition metal d-orbitals are often the key contributors to catalytic activity [86, 97]. Understanding this mechanistic framework is essential for guiding future efforts aimed at enhancing catalytic performance through targeted modifications of the active Fe-chalcogen interface rather than the sublayer composition.

3.5.7 Anomalous Electrochemical Features and Surface Oxidation Behavior

While the initial analysis of the linear sweep voltammetry (LSV) data suggested comparable intrinsic catalytic activities for FGT and FGaT basal planes, a more detailed examination reveals that this interpretation is incomplete. Notably, the LSV curve for FGaT exhibits an

doi:10.6342/NTU202503490

unexpected and distinct peak at approximately -0.4 V versus the reversible hydrogen electrode (RHE) (Figure 03.11). This electrochemical feature, although previously observed in studies involving exfoliated FGT samples [83], has not been thoroughly investigated or explained in the literature to date.

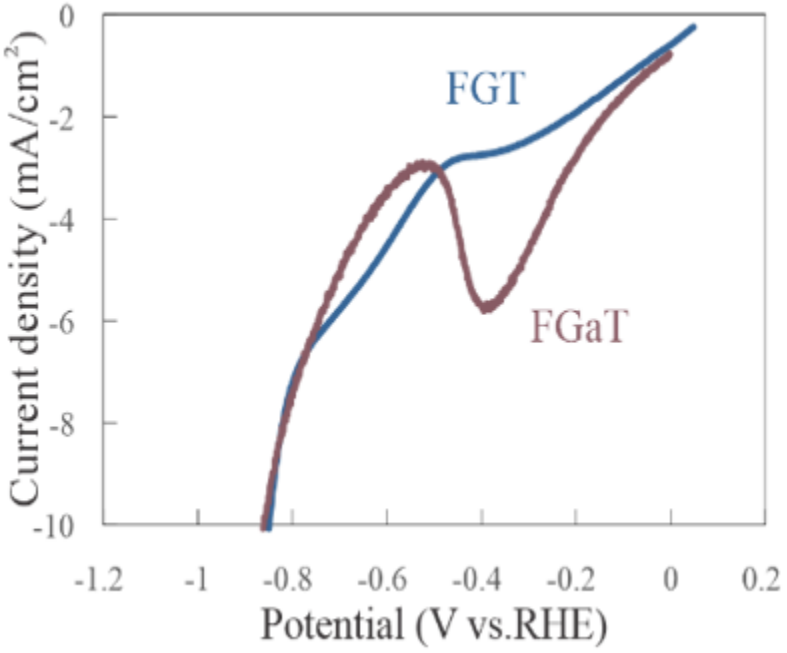

Figure 03.11: LSV curve revealing a distinct peak of FGaT at approximately -0.4 V vs RHE

To elucidate the origin and implications of this anomalous peak, we extended our electrochemical characterization by performing cyclic voltammetry (CV) measurements on both FGT and FGaT under identical conditions in 0.5 M H_2SO_4 electrolyte.

doi:10.6342/NTU202503490

3.5.8 Cyclic Voltammetry (CV) Measurement

Cyclic voltammetry (CV) is a widely utilized electroanalytical technique that provides critical insights into the redox behavior, electron transfer kinetics, electrochemical reversibility, and mass transport properties of a broad range of materials, including metals, semiconductors, coordination complexes, and advanced heterostructures [90, 92]. In a typical CV experiment, the potential applied to the working electrode is swept linearly in a triangular waveform between two set potential limits at a controlled scan rate. This potential modulation induces oxidation or reduction reactions of electroactive species at the electrode–electrolyte interface, generating a current response that is recorded as a function of the applied potential to produce a voltammogram [90]. The shape and characteristics of the voltammogram reveal fundamental electrochemical information: for a reversible redox couple, well-defined anodic and cathodic peaks appear symmetrically with a peak-to-peak separation close to 59/n mV at room temperature, where n is the number of electrons transferred [92]. The peak current (i_p) is governed predominantly by diffusion of the electroactive species and follows the Randles–Ševčík equation, exhibiting a linear dependence on the square root of the scan rate ($\nu^{1/2}$), which confirms diffusion-controlled electron transfer [90, 98]. Deviations from this behavior may indicate surface-confined redox processes, slow electron transfer kinetics, or complex coupled chemical reactions such as adsorption or catalytic transformations [92].

CV's versatility extends to the study of complex electrocatalytic reactions, including the hydrogen evolution reaction (HER), oxygen evolution reaction (OER), and oxygen reduction reaction (ORR), where it serves as a primary tool to probe catalytic activity and stability.

doi:10.6342/NTU202503490

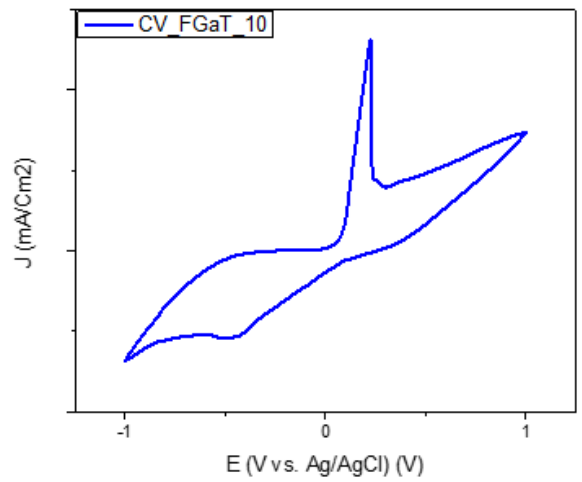

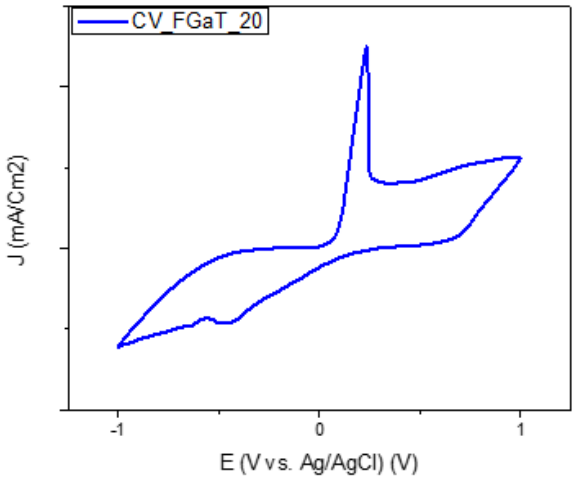

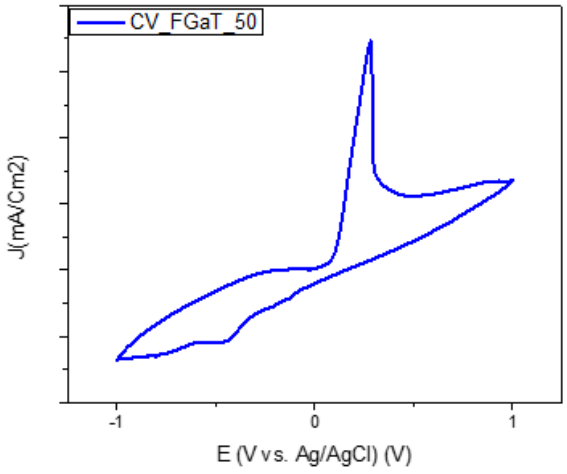

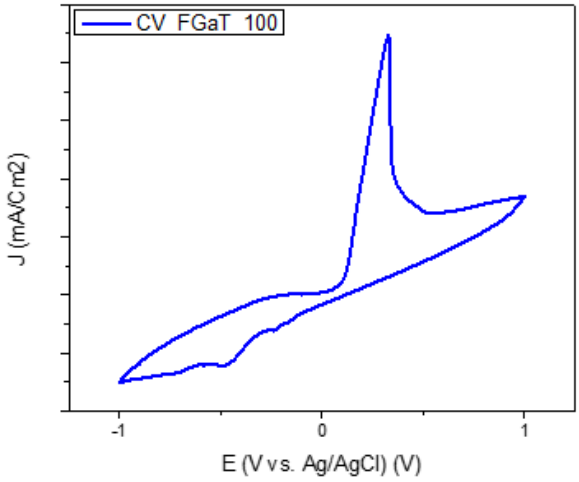

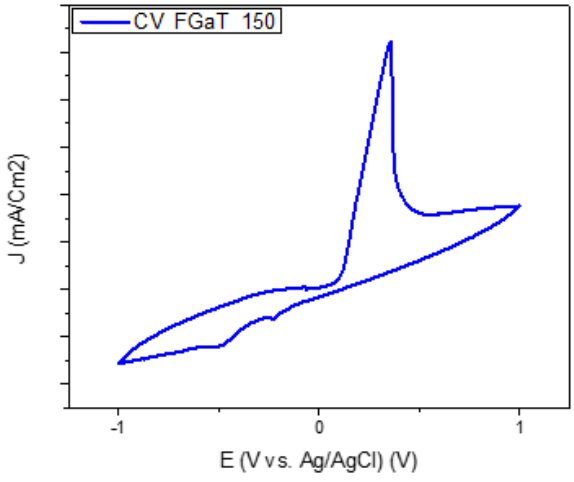

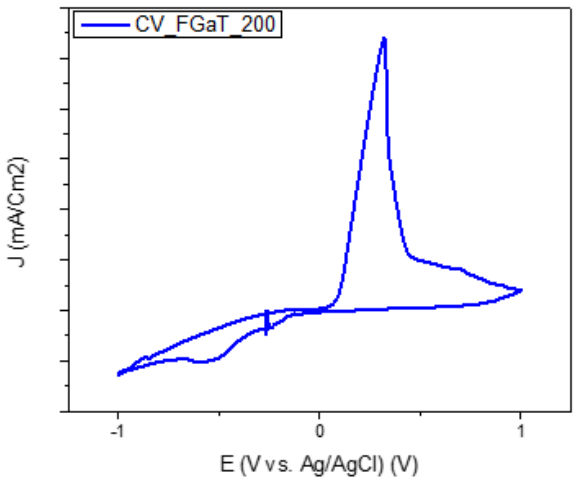

doi:10.6342/NTU202503490

Figure 03.12: Cyclic Voltammetry curve for FGaT at different scan rates (a) 10 mV/Second (b) 20 mV/Second (c) 50 mV/Second (d) 100 mV/Second (e) 150 mV/Second (f) 200 mV/Second

Table 3.1: Oxidation and reduction peak positions of FGaT at different scan rates

Scan Rate	Peak Position Oxidation (Upper Curve)		Peak Position Reduction (Lower Curve)	
	X (Voltage)	Y (mACm-2)	X (Voltage)	Y(mACm-2)
10	0.22384	13095.03139	-0.49997	-5402.76582
20	0.23464	12477.51915	-0.476	-4637.4664
50	0.28274	17351.85147	-0.52546	-5470.51633
100	0.32735	22348.54832	-0.49693	-6100.09618
150	0.35492	26129.55127	-0.53242	-6120.31538
200	0.3195006	26992.2418	-0.59905	-5146.76035

doi:10.6342/NTU202503490

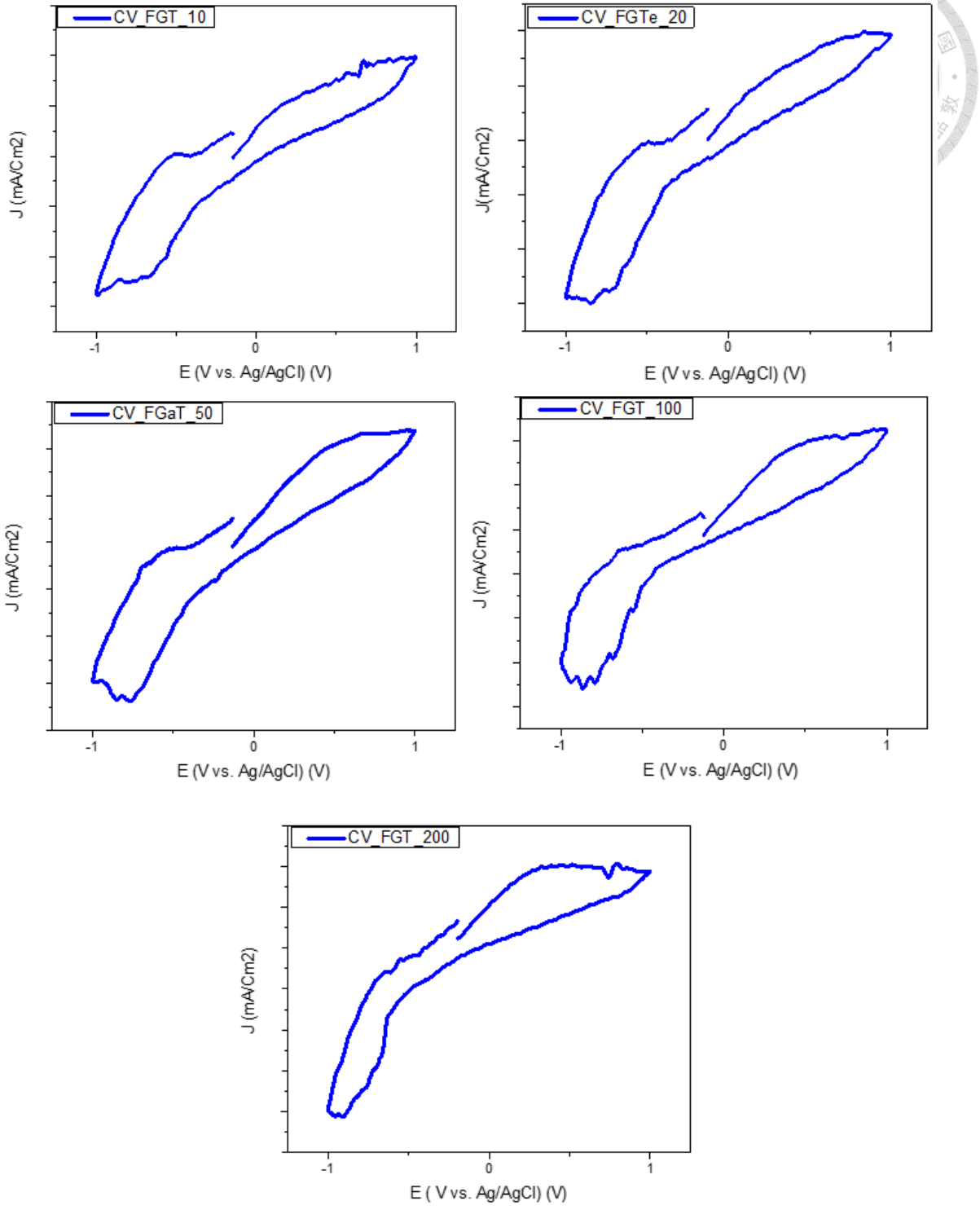

Figure 03.13: Cyclic Voltammetry curve for FGT at different scan rates (a) 10 mV/Second (b) 20 mV/Second (c) 50 mV/Second (d) 100 mV/Second (e) 200 mV/Second

doi:10.6342/NTU202503490

Table 3.2: Oxidation and reduction peak positions of FGT at different scan rates

Scan Rate	Peak Position Oxidation (Upper Curve)		Peak Position Reduction (Lower Curve)	
	X (Voltage)	Y (mACm-2)	X (Voltage)	Y(mACm-2)
10	-0.48507	4.911E-5	-0.80728	-0.00252
20	-0.49369	-3.9969E-5	-0.84683	-0.00299
50	-0.52458	-1.25423E-4	-0.77027	-0.00338
100	-0.6415	-4.65478E-4	-0.86113	-0.00359
200	-0.63899	-5.67081E-4	-0.91178	-0.00413

3.5.9 Comparative CV Study of Fe_3GaTe_2 and Fe_3GeTe_2

To ensure an accurate and meaningful comparison between the two materials, the CV curves were normalized by the capacitive background charge. This normalization accounts for differences in the effective electrochemically active surface area due to variations in crystal size and morphology, thereby allowing us to isolate intrinsic differences in electrochemical behavior.

doi:10.6342/NTU202503490

Capacitive Background Charge in Cyclic Voltammetry:

In cyclic voltammetry (CV) measurements, the total current response consists of both faradaic and non-faradaic components. The non-faradaic current, often referred to as the capacitive current, arises from the charging and discharging of the electrical double layer at the electrode-electrolyte interface. This double layer behaves like a nanoscale capacitor, where charge accumulates electrostatically without involving any electron transfer reactions. The capacitive current i_c is directly proportional to the scan rate (ν) and the double-layer capacitance (C_{dl}), following the relation $i_c = C_{dl} \times \nu$. Consequently, the capacitive background charge, defined as the integral of the capacitive current over the potential window, reflects the total electrostatic charge stored during the CV scan and scales with the electrode surface area and morphology.

Accounting for the capacitive background charge is essential for accurate interpretation of CV data, especially when comparing the intrinsic electrochemical activity of different materials or electrodes with varying surface areas. Normalization of CV curves by the capacitive background charge effectively removes the influence of surface area and capacitance variations, isolating the faradaic current associated with redox processes and catalytic activity [99]. This approach ensures that observed differences in electrochemical responses are due to material properties rather than geometric factors.

The electrical double layer capacitance itself is governed by the structure of the interface, often described by classical models such as the Helmholtz and Gouy-Chapman-Stern models, which consider the compact layer of adsorbed ions and the diffuse ionic layer in the electrolyte [100]. Understanding and quantifying capacitive background charge is therefore

doi:10.6342/NTU202503490

fundamental to electrochemical characterization and the rational design of efficient electrocatalysts.

Normalization of Cyclic Voltammetry Curves by Capacitive Background Charge

Since the capacitive current scales linearly with the electrode surface area and the scan rate, differences in electrode morphology or size can cause variations in the total current response that do not reflect intrinsic material activity. To enable accurate comparison of electrochemical behavior across different samples, it is essential to normalize CV curves by the capacitive background charge.

The normalization procedure involves first identifying a potential region in the CV where no faradaic processes occur (i.e., only capacitive charging is present). The capacitive background charge Q_c is then calculated by integrating the capacitive current over this potential window. Subsequently, the entire CV current or charge is divided by Q_c, effectively removing the influence of surface area and capacitance differences [101]. This approach isolates the faradaic response related to the intrinsic electrochemical properties of the material, allowing for meaningful comparison between electrodes with varying surface areas or morphologies.

Normalization by capacitive background charge is a widely accepted practice in electrochemical characterization to improve reproducibility and interpretability of CV data [102]. It ensures that observed differences in peak currents, onset potentials, or reaction kinetics are due to material properties rather than geometric factors. This technique is particularly important when evaluating catalysts or electrode materials where surface roughness and active site density vary significantly.

doi:10.6342/NTU202503490

The normalized CV profiles of FGT and FGaT were largely similar across the potential window; however, a pronounced deviation was observed in the anodic branch of FGaT (Figure 3.14). This deviation signifies a fundamental difference in the oxidative behavior of the two materials, suggesting that the substitution of Ge by Ga in the sublayer affects the electrochemical stability or reactivity of surface species.

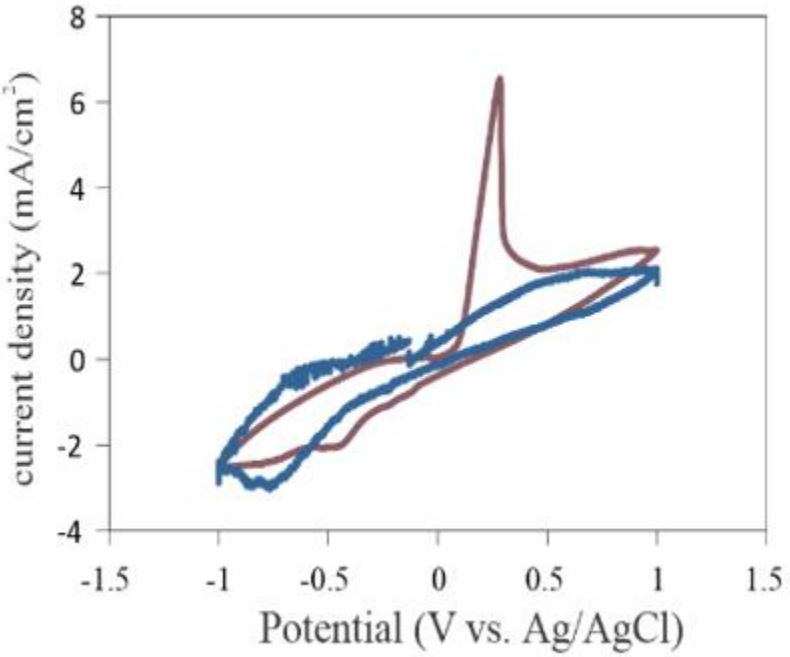

Figure 03.14: Capacitive-background-corrected cyclic voltammetry (CV) curves showing a stronger anodic current response in FGaT

To quantitatively analyze this discrepancy, a semi-derivative analysis of the CV response was conducted (Figure 3.15).

doi:10.6342/NTU202503490

Semi-Derivative Analysis of Cyclic Voltammetry Response

Cyclic voltammetry (CV) is a widely used electrochemical technique to probe redox processes, reaction kinetics, and mechanisms. However, CV curves often exhibit overlapping peaks or broad features, especially in complex systems with multiple electrochemical events occurring at similar potentials. To resolve such complexities and extract more precise quantitative information, semi-derivative analysis (also known as fractional differentiation or semi-differentiation) is employed as a powerful mathematical tool.

Concept and Purpose

Semi-derivative analysis involves calculating the half-order derivative (semi-derivative) of the CV current with respect to potential or time. Unlike the conventional first derivative, the semi-derivative sharpens and narrows the voltametric peaks, improving peak resolution and enabling the separation of closely spaced or overlapping signals [103]. This technique enhances the interpretability of CV data by accentuating features related to diffusion-controlled redox processes while minimizing the influence of background currents or non-diffusion phenomena.

Theoretical Background

The semi-derivative is a concept from fractional calculus, which generalizes the notion of integer-order derivatives to non-integer (fractional) orders. For reversible electrochemical reactions, the semi-derivative of the current response follows theoretical relations consistent with diffusion-controlled processes and exhibits an exponential decay form under ideal conditions [103]. This approach allows the extraction of kinetic parameters such as diffusion coefficients with improved accuracy compared to raw CV data.

doi:10.6342/NTU202503490

Practical Implementation

Data Preparation: Raw CV data (current vs. potential) are first collected under controlled experimental conditions.

Numerical Calculation of Semi-Derivative: The semi-derivative is computed using numerical algorithms based on fractional differentiation formulas. This can be implemented via specialized software or custom scripts in platforms such as MATLAB or Python [103].

Peak Resolution and Analysis: The semi-differentiated CV curve exhibits sharper and narrower peaks than the original voltammogram. This facilitates the separation of overlapping peaks, accurate determination of peak potentials, and quantification of individual electrochemical processes [104].

Mechanistic Insights: Semi-derivative analysis can distinguish diffusion-controlled processes from adsorption or kinetic limitations, as these phenomena produce distinct signatures in the semi-derivative domain [105].

Advantages

Improved Peak Separation: Semi-derivative peaks are narrower and less affected by diffusional tailing, enabling resolution of peaks separated by as little as ~110 mV for reversible one-electron processes at room temperature [104].

Reduced Background Influence: The method minimizes the impact of capacitive or non-faradaic background currents, enhancing signal clarity.

doi:10.6342/NTU202503490

Quantitative Accuracy: Diffusion coefficients and kinetic parameters derived from semi-derivative curves show excellent agreement with classical theoretical models[103].

Applications

Semi-derivative analysis has been successfully applied to:

- Disentangling overlapping redox peaks in complex electrochemical systems [103].
- Mechanistic studies of electrocatalysts and surface-adsorbed species [105].
- Enhancing the precision of electrochemical parameter extraction in both reversible and irreversible reactions [104].

For FGT, three distinct anodic peaks were identified at approximately -0.6 V, -0.2 V, and 0.6 V versus Ag/AgCl reference electrode. These peaks correspond to sequential oxidation states of Fe, reflecting its complex redox chemistry and underscoring the electrochemical significance of Fe centers in governing the material's behavior [106, 107].

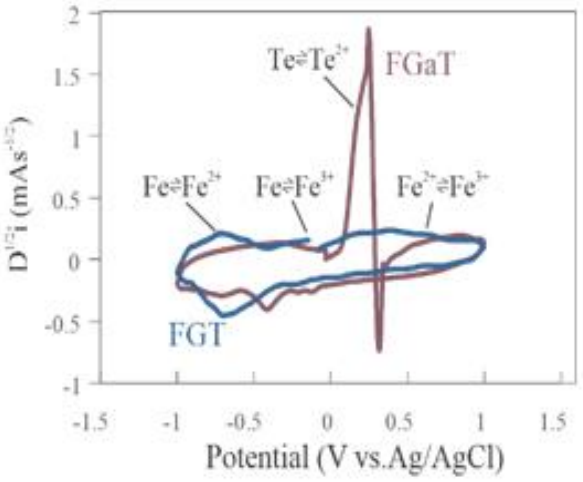

doi:10.6342/NTU202503490

Figure 03.15: Semi-derivative CV analysis identifying key redox transitions in FGT (at -0.6 V, -0.2 V, and 0.6 V) and a Te-related oxidation peak in FGaT at 0.4 V

In contrast, the anodic current response of FGaT was dominated by a single prominent peak centered around 0.4 V vs Ag/AgCl. Based on previous Spectro-electrochemical studies and surface analysis, this peak can be attributed primarily to the oxidation of tellurium (Te) atoms on the surface [108]. This finding is particularly insightful as it indicates that while gallium substitution does not directly participate in the electrochemical reactions, it exerts a significant influence on the chemical environment and stability of surface Te atoms.

The modulation of Te oxidation behavior by Ga incorporation suggests an indirect but crucial role of Ga in altering surface chemistry and possibly the durability of the catalyst under oxidative conditions. This effect may arise from subtle changes in electronic structure or local bonding environments induced by Ga atoms in the sublayer, which in turn affect the oxidation potential and kinetics of surface Te species.

These observations highlight the complex interplay between sublayer composition and surface electrochemical properties. They also emphasize that catalytic performance and stability cannot be fully understood by considering only the basal plane activity or the transition metal centers alone. Instead, the surface chalcogen atoms and their interaction with sublayer elements must be carefully considered, especially for long-term catalyst operation and resistance to oxidative degradation.

3.6 Scan-Rate-Dependent Cyclic Voltammetry to Probe Tellurium Oxidation Reversibility

doi:10.6342/NTU202503490

To further investigate the mechanistic aspects of the anomalous oxidation peak observed in FGaT and to test the hypothesis that surface tellurium (Te) oxidation exhibits limited reversibility, we performed scan-rate-dependent cyclic voltammetry (CV) experiments. This technique is widely employed in electrochemical studies to assess the kinetics and reversibility of redox processes by varying the potential sweep rate and analyzing the corresponding changes in peak characteristics [90].

3.6.1 The Randles–Ševčík Trend in Cyclic Voltammetry

The Randles–Ševčík equation is a foundational expression in electroanalytical chemistry, particularly for interpreting cyclic voltammetry (CV) data in systems where redox processes are governed by diffusion. First derived by Randles (1948) and later refined by Ševčík (1948), this equation quantitatively relates the peak current observed in a cyclic voltammogram to the square root of the scan rate, under the assumption of semi-infinite linear diffusion and reversible electron transfer kinetics [98, 109, 110]. At room temperature (298 K), the Randles–Ševčík equation is typically expressed as:

$$i_p = (2.69 * 10^5) n^{3/2} A D^{1/2} C v^{1/2}$$

Where:

- i_p is the peak current in amperes (A)
- n is the number of electrons transferred in the redox event
- A is the area of the working electrode (cm^2)
- D is the diffusion coefficient of the redox-active species (cm^2/s)
- C is the concentration of the species in solution (mol/cm^3)

doi:10.6342/NTU202503490

- v is the scan rate of the potential sweep (V/s)

The linear dependence of i_p on $\nu^{1/2}$, often termed the Randles–Ševčík trend, serves as a diagnostic indicator of diffusion-controlled, reversible electrochemical behavior. In practical terms, when a series of CVs is recorded at increasing scan rates, a plot of i_p vs. $\nu^{1/2}$ should yield a straight line, confirming that the redox process is limited by the diffusion of species to the electrode surface rather than by kinetic or surface phenomena [92, 110].

This linear relationship is particularly valuable in distinguishing between diffusion-controlled and surface-confined processes. Deviations from this trend, such as non-linearity or changes in slope, can indicate the presence of kinetic limitations (quasi-reversible or irreversible systems), significant adsorption of redox species, coupled chemical reactions (e.g., EC or ECE mechanisms), or alterations in the electrode surface area due to morphological changes or degradation [91, 110] . In the context of materials research, such as studies involving FGaT and FGT single crystals, the Randles–Ševčík analysis is instrumental in evaluating the electrochemical response before and after treatments like exposure to acidic media (e.g., 0.5 M H_2SO_4 during hydrogen evolution reaction (HER) studies). A consistent Randles–Ševčík trend prior to treatment suggests a stable and homogeneous electrochemical interface, while the persistence of this trend after HER cycling or chemical etching indicates that the redox processes remain predominantly diffusion-controlled, despite possible surface modifications [92].

Furthermore, the slope of the Randles–Ševčík plot can be used to extract the diffusion coefficient of the redox-active species, providing quantitative insight into the transport properties within the system. This approach, when combined with complementary techniques

doi:10.6342/NTU202503490

such as microscopy or spectroscopy, offers a comprehensive understanding of how structural and surface changes influence electrochemical behavior [91, 110]. Overall, the Randles–Ševčík equation remains a powerful tool for diagnosing and quantifying the fundamental processes that govern electrochemical systems.

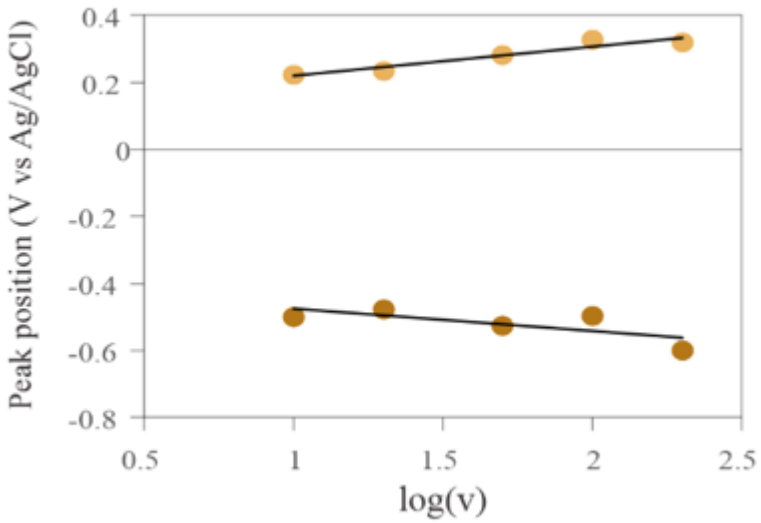

Figure 03.16: CVs at different scan rates, showing increasing peak separation with scan rate, indicating kinetic limitations

As the scan rate was systematically increased, we observed a progressive widening of the peak separation between the anodic and cathodic currents for both FGT and FGaT samples (Figure 03.16). This increase in peak-to-peak separation is a classical indicator of kinetic limitations in the electron transfer process, suggesting that the oxidation and reduction reactions of surface species do not proceed with equal facility or speed. Such behavior often points to quasi-reversible or irreversible electrochemical processes, where the rate of electron transfer or coupled chemical reactions restricts the electrochemical response at higher scan rates [111].

doi:10.6342/NTU202503490

To quantitatively analyze this phenomenon, the peak currents from both the oxidation and reduction branches were plotted against the scan rate (Figure 03.17).

3.6.2 Diffusion-Controlled Potential Shift

In cyclic voltammetry, the potential separation between oxidation (E_pa) and reduction (E_pc) peaks provides critical insights into electron transfer kinetics and mass transport limitations. For fully reversible systems at 298 K, the theoretical peak separation ΔE_p = E_pa - E_pc equals 59/n mV, where n is the number of electrons transferred, a hallmark of Nernstian behavior governed by fast electron transfer kinetics relative to mass transport [90]. However, as scan rates increase or systems exhibit quasi-reversible characteristics, this ideal separation deviates due to diffusion-controlled potential shifts. At elevated scan rates (>100 mV/s), the finite time for reactant diffusion creates steep concentration gradients near the electrode surface, requiring increased overpotentials to drive the reaction [92]. These manifests as anodic peaks shifting positively and cathodic peaks shifting negatively relative to the formal potential (E^0), a phenomenon quantitatively described by Laviron's model for quasi-reversible systems [111].

$$E_p = E^0 + \frac{RT}{\alpha nF}[\ln\left(\frac{RTk^0}{\alpha nF}\right) + lnv]$$

Where:

- E_p is the peak potential
- E^0 formal redox potential
- R is Universal Gas Constant 8.314 $J \cdot mol^{-1} \cdot K^{-1}$
- T is absolute temperature in kelvin (K)

doi:10.6342/NTU202503490

- F is the Faraday constant, equal to approximately 96485 $C \cdot mol^{-1}$
- α is the charge transfer coefficient
- k^0 is the heterogeneous rate constant
- ν is the scan rate

The linear relationship between E_p and lnν allows extraction of kinetic parameters: the slope provides αn, while the y-intercept yields k^0 when E^0 is known [91]. In materials studies, such as with FGaT or FGT single crystals, these shifts reveal dynamic interfacial changes. For instance, after acidic treatments (e.g., 0.5 M H_2SO_4 exposure), increased peak separations at high scan rates may indicate surface roughening or kinetic degradation, while maintained linear E_p vs. ln ν dependence suggests preserved diffusion control [92]. This analysis complements Randles-Ševčík evaluations and electrochemical impedance spectroscopy, providing a multi-parametric view of charge transfer efficiency in energy materials.

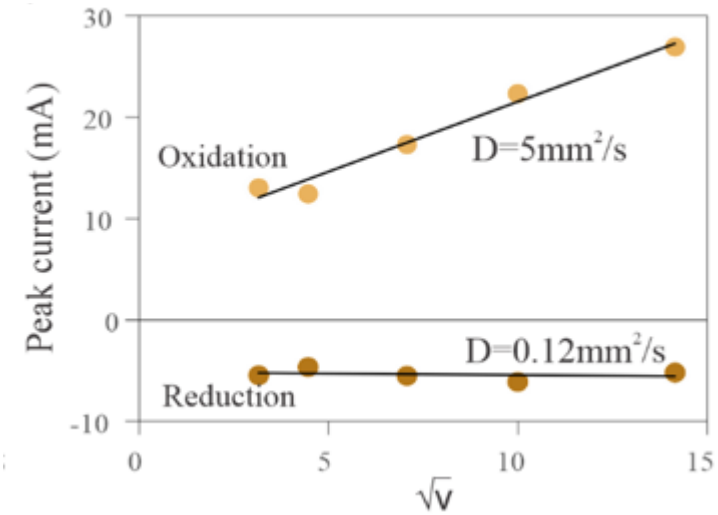

Figure 03. 17: Scan rate–dependent analysis of peak current, revealing diffusion-limited and irreversible oxidation behavior

doi:10.6342/NTU202503490

This analysis revealed a marked difference in the dependence of peak current on scan rate between the two branches. Specifically, the oxidation peak current exhibited a nearly linear relationship with scan rate, indicative of a surface-controlled process or fast electron transfer kinetics. In contrast, the reduction peak current showed a distinctly different trend, suggesting slower kinetics or diffusion limitations.

Using this relationship, the diffusion coefficients for the oxidation and reduction processes were estimated. Remarkably, the diffusion coefficient associated with the oxidation process was found to be approximately 50 times greater than that for the reduction process. This large disparity confirms that the oxidation of Te on the surface is kinetically favored and relatively facile, whereas the subsequent reduction is significantly hindered, indicating an irreversible or strongly quasi-reversible redox process [112].

The irreversibility of Te oxidation has important implications for the electrochemical stability and catalytic performance of FGaT. It suggests that once oxidized, surface Te species may not readily revert to their original state under reductive conditions, potentially leading to surface degradation or passivation during prolonged electrochemical operation. This behavior contrasts with more reversible redox couples where oxidation and reduction occur readily and symmetrically.

These findings align with previous studies of chalcogenide surfaces where oxidation processes often involve complex structural or chemical changes that limit reversibility. Understanding these kinetic constraints is essential for developing strategies to enhance catalyst durability, such as surface passivation, protective coatings, or compositional tuning to stabilize surface chalcogen species.

doi:10.6342/NTU202503490

3.7 Theoretical and Experimental Investigation of Tellurium Vacancy Formation and Material Stability

To elucidate the underlying reasons for the observed greater electrochemical instability of FGaT compared to FGT, we turned to first-principles density functional theory (DFT) calculations aimed at quantifying the energetics associated with tellurium (Te) vacancy formation in both materials. Understanding vacancy formation energies is critical because the ease with which Te atoms can be removed from the lattice directly influences surface stability, catalytic durability, and susceptibility to degradation under electrochemical conditions.

3.7.1 Computational Approach

Using experimentally determined lattice parameters as the starting point, we constructed single unit cell models of pristine FGT and FGaT. The total energies of these pristine configurations, denoted as E_{pristine}, were calculated to serve as reference states. To simulate Te vacancy formation, we generated defective structures by removing a single Te atom from the unit cell and recalculating the total energy, $E_{\text{deficient}}$. Additionally, the energy of an isolated Te atom, E_{Te}, was computed to represent the reference energy of the removed atom.

The formation energy of a Te vacancy, ΔE, was then determined using the following equation:

$$\Delta E = E_{pristine} - E_{deficient} - E_{Te}$$

doi:10.6342/NTU202503490

This formulation effectively captures the energetic cost of removing a Te atom from the lattice and placing it in an isolated state, providing a quantitative measure of the atom's binding strength within the crystal.

3.7.2 Results and Interpretation

Our DFT calculations revealed that the vacancy formation energy for Te in FGaT is approximately 4.16 eV, while in FGT it is higher, at about 4.36 eV. The difference of 0.20 eV (200 meV) indicates that Te atoms are weaklier bound in the Ga-substituted structure. This reduced binding energy suggests that Te atoms in FGaT are more susceptible to removal or loss under oxidative electrochemical conditions, thereby contributing to the material's decreased stability.

The weaker Te binding in FGaT can be attributed to subtle electronic and structural modifications induced by gallium substitution in the sublayer. Ga atoms may alter the local bonding environment or electronic charge distribution, weakening the Te-metal interactions and facilitating vacancy formation.

3.7.3 Experimental Validation

To experimentally validate these theoretical predictions, we subjected both FGT and FGaT samples to prolonged electrochemical cycling in acidic electrolyte, simulating extended operational conditions. The performance degradation was monitored by measuring changes in catalytic activity and electrochemical response over time.

doi:10.6342/NTU202503490

As shown in Figure 03.18, FGT exhibited significantly better stability, maintaining a higher fraction of its initial catalytic performance after extended cycling. In contrast, FGaT showed pronounced degradation, consistent with the theoretical prediction of easier Te loss.

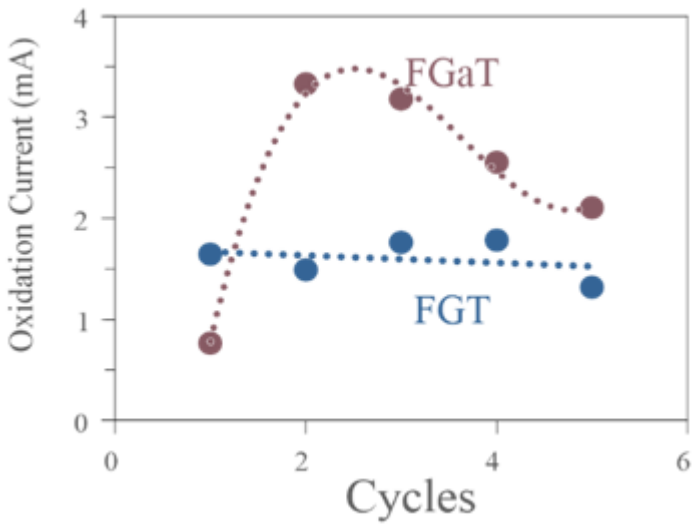

Figure 03.18: Cycling data comparing performance degradation in FGT and FGaT

Post-mortem optical microscopy provided further evidence supporting these findings. The FGaT samples displayed visible physical damage and surface deterioration after cycling (Figure 03.19), indicative of structural breakdown likely caused by Te vacancy formation and subsequent lattice destabilization. Conversely, FGT samples retained their structural integrity to a much greater extent.

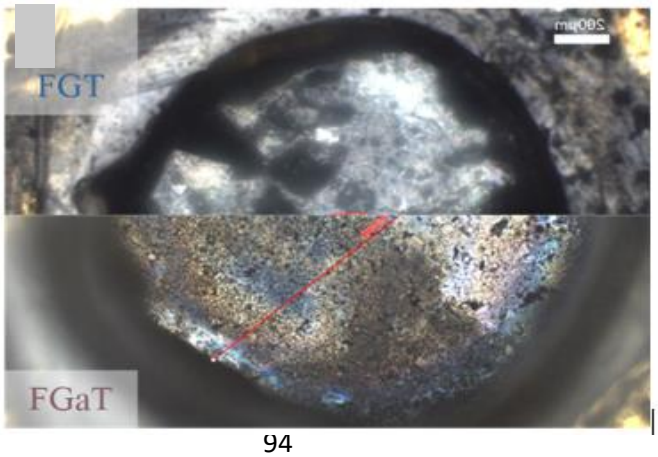

doi:10.6342/NTU202503490

Figure 03.19: Horizontally split arrangement of two optical microscopy images post-cycling, showing retention of flat surface in the FGT case (top) and visible degradation in FGaT (bottom), consistent with surface corrosion

3.8 Implications

These combined theoretical and experimental results underscore the critical role of Te vacancy formation energy in determining the electrochemical stability of layered chalcogenides. The substitution of Ge by Ga, while not significantly affecting basal-plane catalytic activity, compromises the structural robustness by weakening Te binding. This insight is vital for guiding the design of more durable catalysts, suggesting that strategies to strengthen chalcogen binding or prevent vacancy formation could enhance long-term performance.

doi:10.6342/NTU202503490

doi:10.6342/NTU202503490

CHAPTER: 04

CONCLUSION – SUMMARY OF FINDINGS, IMPLICATIONS, AND SUGGESTIONS FOR FUTURE RESEARCH

4.1 Conclusions

This study presents a comprehensive comparative investigation of two novel layered magnetic materials, Fe_3GeTe_2 (FGT) and Fe_3GaTe_2 (FGaT), focusing on their structural, electrochemical, and stability properties within the context of hydrogen evolution reaction (HER) catalysis and magneto-electrochemical applications.

Through detailed diffraction and high-resolution microscopy analyses, we confirmed the strong structural and morphological resemblance between FGT and FGaT, affirming their status as structural homologs within the family of layered transition-metal chalcogenides. Surface characterization further revealed that both materials possess nearly identical surface topographies, a key factor influencing their electrochemical behavior. This similarity in surface structure correlates with their comparable HER catalytic activities, predominantly governed by the redox behavior of iron atoms embedded in their layered lattices. These findings underscore the critical role of the Fe coordination environment in driving catalytic performance.

Despite their analogous catalytic efficiencies, a marked difference in long-term electrochemical stability was observed. FGaT exhibited significantly reduced stability relative to FGT under identical testing conditions. Theoretical calculations and structural modeling attributed this disparity to a thermodynamically less stable tellurium environment

doi:10.6342/NTU202503490

in the gallium-substituted compound. The substitution of Ga for Ge alters the electronic environment, modifying the binding energy landscape and increasing the material's vulnerability to degradation during extended electrochemical operation.

These insights deepen our understanding of the intricate structure–property–stability relationships in magnetic two-dimensional materials and highlight the profound impact of atomic-level substitutions on tuning material performance. Our results not only demonstrate the potential of structural homologs like FGT and FGaT for advanced electrocatalysis and spintronic interface applications but also emphasize the necessity of balancing catalytic activity with intrinsic material stability, particularly in systems that couple magnetic and electrochemical functionalities.

In the broader scope of magneto-electrochemistry, this work reinforces the importance of integrating morphological and thermodynamic considerations when designing and selecting candidate materials. As the field progresses toward the practical integration of 2D magnets in energy conversion technologies, our findings highlight the dual role of transition-metal centers in dictating both magnetic and catalytic properties, as well as the trade-offs introduced by compositional tuning.

4.2 Future Work

Building on the insights gained from this study, several promising avenues for future research are proposed to further advance the understanding and application of layered magnetic materials in electrocatalysis and magneto-electrochemistry:

1. **Investigation of Oxygen Evolution Reaction (OER) Under Magnetic Fields**

doi:10.6342/NTU202503490

- Recent studies have demonstrated that applying an external magnetic field can significantly enhance the kinetics of the oxygen evolution reaction (OER) on ferromagnetic catalysts by promoting spin-polarized electron transfer, particularly at the initial electron transfer step[19, 113]. Exploring the OER activity of Fe_3GeTe_2 (FGT) and Fe_3GaTe_2 (FGaT) under controlled magnetic fields could reveal new mechanisms of catalytic enhancement and provide a direct comparison with their HER performance.
- In situ techniques, such as X-ray emission spectroscopy, can be employed to probe the spin states of active sites during OER, offering atomic-level insights into the interplay between magnetic ordering and catalytic activity [113].

2. Cobalt Doping for Enhanced Magnetic and Electrocatalytic Properties

- Cobalt doping has been shown to significantly influence the crystallinity, stability, and magnetic properties of iron-based materials, often increasing coercivity, magnetic anisotropy, and overall stability [114]. Introducing cobalt into the FGT and FGaT lattices may yield materials with improved long-term electrochemical stability and tunable magnetic properties, which are beneficial for both HER and OER.
- Cobalt incorporation can also induce pronounced spin polarization, as observed in CoIr and CoFe-based catalysts, leading to enhanced OER activity, particularly under magnetic fields [113, 115]. Systematic studies on the optimal cobalt doping concentration and its impact on both catalytic activity and magnetic response are warranted.

doi:10.6342/NTU202503490

3. Outlook: Integration and Device-Level Applications

- The dual functionality of these materials as both magnetic and electrocatalytic components positions them as strong candidates for next-generation magneto-electrochemical devices, including spintronic energy conversion systems and multifunctional electrodes.
- Future work should also address the scalability, device integration, and operational stability of cobalt-doped FGT/FGaT materials in realistic electrochemical environments, especially under simultaneous magnetic and electrochemical stimuli.

4. Mechanistic Studies and Theoretical Modeling

- Advanced computational modeling, including density functional theory (DFT), can be leveraged to predict the effects of magnetic field and cobalt substitution on the electronic structure, binding energies, and reaction pathways of these layered materials [115].
- Mechanistic studies should focus on correlating experimental observations with theoretical predictions to establish design principles for tailoring spin-polarized electrocatalysts.

Pursuing these directions will not only deepen the fundamental understanding of magnetically enhanced electrocatalysis but also accelerate the development of robust, high-performance materials for sustainable energy technologies.

doi:10.6342/NTU202503490

REFERENCES

[1] J. Masa, C. Andronescu, and W. Schuhmann, "Electrocatalysis as the nexus for sustainable renewable energy: the gordian knot of activity, stability, and selectivity," *Angewandte Chemie International Edition*, vol. 59, no. 36, pp. 15298–15312, 2020.

[2] Q. Jiang, K. Jiang, Y. Ye, K. Xi, and C. Xia, "Electrocatalysis Towards Carbon-Neutral Future," vol. 11, ed: Frontiers Media SA, 2023, p. 1159716.

[3] T. Binninger *et al.*, "Thermodynamic explanation of the universal correlation between oxygen evolution activity and corrosion of oxide catalysts," *Scientific reports,* vol. 5, no. 1, p. 12167, 2015.

[4] T. Schuler, T. Kimura, T. J. Schmidt, and F. N. Büchi, "Towards a generic understanding of oxygen evolution reaction kinetics in polymer electrolyte water electrolysis," *Energy & Environmental Science*, vol. 13, no. 7, pp. 2153–2166, 2020.

[5] F. M. Fernandes, N. F. Xavier Jr, G. F. Bauerfeldt, M. S. Pereira, and C. O. da Silva, "Thermodynamic and kinetic analysis of the oxygen evolution reaction on TiO2 (100) and (101) surfaces: A DFT study," *Surface Science*, vol. 753, p. 122654, 2025.

[6] J. Zhang *et al.*, "Advances in thermodynamic-kinetic model for analyzing the oxygen evolution reaction," *Acs Catalysis,* vol. 10, no. 15, pp. 8597–8610, 2020.

[7] J. Geppert, F. Kubannek, P. Röse, and U. Krewer, "Identifying the oxygen evolution mechanism by microkinetic modelling of cyclic voltammograms," *Electrochimica Acta,* vol. 380, p. 137902, 2021.

[8] J. Yu *et al.*, "A survey of Earth-abundant metal oxides as oxygen evolution electrocatalysts in acidic media (pH< 1)," *Ees Catalysis*, vol. 1, no. 5, pp. 765–773, 2023.

doi:10.6342/NTU202503490

[9] J. Yu *et al.*, "Sustainable oxygen evolution electrocatalysis in aqueous 1 M H2SO4 with earth abundant nanostructured Co3O4," *Nature communications*, vol. 13, no. 1, p. 4341, 2022.

[10] M. Huynh, T. Ozel, C. Liu, E. C. Lau, and D. G. Nocera, "Design of template-stabilized active and earth-abundant oxygen evolution catalysts in acid," *Chemical science*, vol. 8, no. 7, pp. 4779–4794, 2017.

[11] H. An, W. Park, H. Shin, and D. Y. Chung, "Recommended practice for measurement and evaluation of oxygen evolution reaction electrocatalysis," *EcoMat*, vol. 6, no. 10, p. e12486, 2024.

[12] M. Risch, "Reporting activities for the oxygen evolution reaction," *Communications Chemistry*, vol. 6, no. 1, p. 221, 2023.

[13] Y. Nosaka, "Molecular mechanisms of oxygen evolution reactions for artificial photosynthesis," *Oxygen*, vol. 3, no. 4, pp. 407–451, 2023.

[14] A. Bund, S. Koehler, H. Kuehnlein, and W. Plieth, "Magnetic field effects in electrochemical reactions," *Electrochimica Acta*, vol. 49, no. 1, pp. 147–152, 2003.

[15] L. Zhang, D. Wu, and X. Yan, "Applications of magnetic field for electrochemical energy storage," *Applied Physics Reviews*, vol. 9, no. 3, 2022.

[16] N. Karki, F. L. Mufoyongo, and A. J. Wilson, "Utilizing the magnetic properties of electrodes and magnetic fields in electrocatalysis," *Inorganic Chemistry Frontiers*, vol. 11, no. 17, pp. 5414–5434, 2024.

[17] S. Luo, K. Elouarzaki, and Z. J. Xu, "Electrochemistry in magnetic fields," *Angewandte Chemie International Edition*, vol. 61, no. 27, p. e202203564, 2022.

doi:10.6342/NTU202503490

[18] W. Yulong, Z. Luo, H. Cui, K. Feng, and C. Yang, "The enhancing effect of magnetic field on the electrochemical ion transport process."

[19] X. Ren *et al.*, "Spin-polarized oxygen evolution reaction under magnetic field," *Nature communications*, vol. 12, no. 1, p. 2608, 2021.

[20] F. Blumenschein *et al.*, "Spin-dependent charge transfer at chiral electrodes probed by magnetic resonance," *Physical Chemistry Chemical Physics*, vol. 22, no. 3, pp. 997–1002, 2020.

[21] X. Wang *et al.*, "Direct control of electron spin at an intrinsically chiral surface for highly efficient oxygen reduction reaction," *Proceedings of the National Academy of Sciences*, vol. 122, no. 9, p. e2413609122, 2025.

[22] P. Vensaus, Y. Liang, J.-P. Ansermet, J. Fransson, and M. Lingenfelder, "Spin-Polarized Electron Transport Promotes the Oxygen Reduction Reaction," 2025.

[23] J. Ying, J.-B. Chen, Y.-X. Xiao, S. I. C. de Torresi, K. I. Ozoemena, and X.-Y. Yang, "Recent advances in Ru-based electrocatalysts for oxygen evolution reaction," *Journal of Materials Chemistry A*, vol. 11, no. 4, pp. 1634–1650, 2023.

[24] C. Wang, F. Yang, and L. Feng, "Recent advances in iridium-based catalysts with different dimensions for the acidic oxygen evolution reaction," *Nanoscale Horizons*, vol. 8, no. 9, pp. 1174–1193, 2023.

[25] Y. Lin *et al.*, "Recent advances in catalysts toward alkaline oxygen evolution reaction (OER)," *Environmental Chemistry and Safety*, 2025.

[26] X. Chen *et al.*, "Research advances in earth-abundant-element-based electrocatalysts for oxygen evolution reaction and oxygen reduction reaction," *Energy Materials*, vol. 3, no. 4, pp. N/A–N/A, 2023.

doi:10.6342/NTU202503490

[27] F. A. Garcés-Pineda, M. Blasco-Ahicart, D. Nieto-Castro, N. López, and J. R. Galán-Mascarós, "Direct magnetic enhancement of electrocatalytic water oxidation in alkaline media," *Nature Energy*, vol. 4, no. 6, pp. 519–525, 2019.

[28] E. van der Minne *et al.*, "The effect of intrinsic magnetic order on electrochemical water splitting," *Applied Physics Reviews*, vol. 11, no. 1, 2024.

[29] S. Li *et al.*, "Recent advances in the development of single atom catalysts for oxygen evolution reaction," *International Journal of Hydrogen Energy*, vol. 82, pp. 1081–1100, 2024.

[30] C. Fang, J. Zhou, L. Zhang, W. Wan, Y. Ding, and X. Sun, "Synergy of dual-atom catalysts deviated from the scaling relationship for oxygen evolution reaction," *Nature Communications*, vol. 14, no. 1, p. 4449, 2023.

[31] Z. Yuan *et al.*, "Enhanced oxygen evolution kinetics via single-atom catalyst design: A review," *Advanced Materials Interfaces*, p. 2400916, 2025.

[32] C. Rong, X. Huang, H. Arandiyan, Z. Shao, Y. Wang, and Y. Chen, "Advances in oxygen evolution reaction electrocatalysts via direct oxygen–oxygen radical coupling pathway," *Advanced Materials*, vol. 37, no. 9, p. 2416362, 2025.

[33] Z. Chen, X. Duan, W. Wei, S. Wang, and B.-J. Ni, "Recent advances in transition metal-based electrocatalysts for alkaline hydrogen evolution," *Journal of Materials Chemistry A*, vol. 7, no. 25, pp. 14971–15005, 2019.

[34] S. Li, E. Li, X. An, X. Hao, Z. Jiang, and G. Guan, "Transition metal-based catalysts for electrochemical water splitting at high current density: current status and perspectives," *Nanoscale*, vol. 13, no. 30, pp. 12788–12817, 2021.

doi:10.6342/NTU202503490

[35] W. Xiong, H. Yin, T. Wu, and H. Li, "Challenges and opportunities of transition metal oxides as electrocatalysts," *Chemistry–A European Journal*, vol. 29, no. 5, p. e202202872, 2023.

[36] H. Yang, N. An, Z. Kang, P. W. Menezes, and Z. Chen, "Understanding Advanced Transition Metal-Based Two Electron Oxygen Reduction Electrocatalysts from the Perspective of Phase Engineering," *Advanced Materials*, vol. 36, no. 25, p. 2400140, 2024.

[37] H. Wang *et al.*, "Enhancing the electrochemical activity of 2D materials edges through oriented electric fields," *ACS nano*, vol. 18, no. 30, pp. 19828–19835, 2024.

[38] A. V. Papavasileiou, M. Menelaou, K. J. Sarkar, Z. Sofer, L. Polavarapu, and S. Mourdikoudis, "Ferromagnetic elements in two-dimensional materials: 2D magnets and beyond," *Advanced Functional Materials*, vol. 34, no. 2, p. 2309046, 2024.

[39] P. Huang, P. Zhang, S. Xu, H. Wang, X. Zhang, and H. Zhang, "Recent advances in two-dimensional ferromagnetism: materials synthesis, physical properties and device applications," *Nanoscale*, vol. 12, no. 4, pp. 2309–2327, 2020.

[40] Y. Yin, X. Kang, and B. Han, "Two-dimensional materials: synthesis and applications in the electro-reduction of carbon dioxide," *Chem. Synth*, vol. 2, no. 4, p. 19, 2022.

[41] S. Noreen *et al.*, "Emerging 2D-Nanostructured materials for electrochemical and sensing Application-A review," *International Journal of Hydrogen Energy*, vol. 47, no. 2, pp. 1371–1389, 2022.

[42] C. Ke, J. Huang, and S. Liu, "Two-dimensional ferroelectric metal for electrocatalysis," *Materials Horizons*, vol. 8, no. 12, pp. 3387–3393, 2021.

doi:10.6342/NTU202503490

[43] B. Behera, B. C. Sutar, and N. R. Pradhan, "Recent progress on 2D ferroelectric and multiferroic materials, challenges, and opportunity," *Emergent Materials,* vol. 4, no. 4, pp. 847–863, 2021.

[44] S. Jiang, Y. Wang, and G. Zheng, "Two-Dimensional Ferroelectric Materials: From Prediction to Applications," *Nanomaterials,* vol. 15, no. 2, p. 109, 2025.

[45] Y. Zhao, J. Gu, and Z. Chen, "Oxygen Evolution Reaction on 2D Ferromagnetic Fe3GeTe2: Boosting the Reactivity by the Self-Reduction of Surface Hydroxyl," *Advanced Functional Materials,* vol. 29, no. 44, p. 1904782, 2019.

[46] Z. Fei *et al.*, "Two-dimensional itinerant ferromagnetism in atomically thin Fe3GeTe2," *Nature materials,* vol. 17, no. 9, pp. 778–782, 2018.

[47] Y. Deng *et al.*, "Gate-tunable room-temperature ferromagnetism in two-dimensional Fe3GeTe2," *Nature,* vol. 563, no. 7729, pp. 94–99, 2018.

[48] C. Tan *et al.*, "Hard magnetic properties in nanoflake van der Waals Fe3GeTe2," *Nature communications,* vol. 9, no. 1, p. 1554, 2018.

[49] R. Roy and R. Mondal, "Anisotropic magnetic, magnetocaloric properties, and critical behavior studies of CVT-grown single-crystalline Fe 3− x GeTe 2," *Physical Review B,* vol. 109, no. 2, p. 024416, 2024.

[50] R. Roemer *et al.*, "Unraveling the electronic structure and magnetic transition evolution across monolayer, bilayer, and multilayer ferromagnetic Fe3GeTe2," *npj 2D Materials and Applications,* vol. 8, no. 1, p. 63, 2024.

[51] Y. Li *et al.*, "Spin-dependent electron transfer in electrochemically transparent van der Waals heterostructures for oxygen evolution reaction," *Materials Science and Engineering: R: Reports,* vol. 161, p. 100856, 2024.

doi:10.6342/NTU202503490

[52] H. Algaidi *et al.*, "Magnetic critical behavior of van der Waals Fe3GaTe2 with above-room-temperature ferromagnetism," *APL Materials*, vol. 12, no. 1, 2024.

[53] Y. You, J. Liu, B. Ding, F. Xu, and Z. Sun, "Critical behavior and anisotropic magnetocaloric effect in off-stoichiometric van der Waals ferromagnet Fe3-xGaTe2," *Journal of Magnetism and Magnetic Materials*, vol. 623, p. 172997, 2025.

[54] Y. Li *et al.*, "Visualizing the effect of oxidation on magnetic domain behavior of nanoscale Fe3GeTe2 for applications in spintronics," *ACS Applied Nano Materials*, vol. 6, no. 6, pp. 4390–4397, 2023.

[55] S. T. Chyczewski *et al.*, "Probing antiferromagnetism in exfoliated Fe 3 GeTe 2 using magneto-transport measurements," *Nanoscale*, vol. 15, no. 34, pp. 14061–14067, 2023.

[56] A. Puthirath Balan *et al.*, "Harnessing Van der Waals CrPS4 and Surface Oxides for Nonmonotonic Preset Field Induced Exchange Bias in Fe3GeTe2," *ACS nano*, vol. 18, no. 11, pp. 8383–8391, 2024.

[57] Z. Chen *et al.*, "Vacancy occupation-driven polymorphic transformation in cobalt ditelluride for boosted oxygen evolution reaction," *ACS nano*, vol. 14, no. 6, pp. 6968–6979, 2020.

[58] M. D. Albaqami *et al.*, "Controlled fabrication of various nanostructures iron-based tellurides as highly performed oxygen evolution reaction," *International Journal of Hydrogen Energy*, vol. 60, pp. 593–600, 2024.

[59] J. Suntivich, K. J. May, H. A. Gasteiger, J. B. Goodenough, and Y. Shao-Horn, "A perovskite oxide optimized for oxygen evolution catalysis from molecular orbital principles," *Science*, vol. 334, no. 6061, pp. 1383–1385, 2011.

doi:10.6342/NTU202503490

[60] Q. H. Wang, K. Kalantar-Zadeh, A. Kis, J. N. Coleman, and M. S. Strano, "Electronics and optoelectronics of two-dimensional transition metal dichalcogenides," *Nature nanotechnology*, vol. 7, no. 11, pp. 699–712, 2012.

[61] A. Sivanesan *et al.*, "Electrochemical pathway for the quantification of SERS enhancement factor," *Electrochemistry communications*, vol. 49, pp. 103–106, 2014.

[62] A. M. Ruiz, D. L. Esteras, D. López-Alcalá, and J. J. Baldoví, "On the origin of the above-room-temperature magnetism in the 2D van der Waals Ferromagnet Fe3GaTe2," *Nano Letters*, vol. 24, no. 26, pp. 7886–7894, 2024.

[63] C. Gong *et al.*, "Discovery of intrinsic ferromagnetism in two-dimensional van der Waals crystals," *Nature*, vol. 546, no. 7657, pp. 265–269, 2017.

[64] B. Huang *et al.*, "Layer-dependent ferromagnetism in a van der Waals crystal down to the monolayer limit," *Nature*, vol. 546, no. 7657, pp. 270–273, 2017.

[65] M. Bonilla *et al.*, "Strong room-temperature ferromagnetism in VSe2 monolayers on van der Waals substrates," *Nature nanotechnology*, vol. 13, no. 4, pp. 289–293, 2018.

[66] J. K. Nørskov *et al.*, "Trends in the exchange current for hydrogen evolution," *Journal of The Electrochemical Society*, vol. 152, no. 3, p. J23, 2005.

[67] M. Binnewies, R. Glaum, M. Schmidt, and P. Schmidt, "Crystal Growth Via the Gas Phase by Chemical Vapor Transport Reactions," *Handbook of solid state chemistry*, vol. 639, pp. 228–305, 2017.

[68] M. Binnewies, M. Schmidt, and P. Schmidt, "Chemical vapor transport reactions–arguments for choosing a suitable transport agent," *Zeitschrift für anorganische und allgemeine Chemie*, vol. 643, no. 21, pp. 1295–1311, 2017.

doi:10.6342/NTU202503490

[69] D. Dimitrov *et al.*, "NbSe2 crystals growth by bromine transport," *Coatings*, vol. 13, no. 5, p. 947, 2023.

[70] R. Heinemann and P. Schmidt, "Crystal Growth by Chemical Vapor Transport: Process Screening by Complementary Modeling and Experiment," *Crystal Growth & Design*, vol. 20, no. 9, pp. 5986–6000, 2020.

[71] R. Sai, O. Gorochov, E. A. Alghamdi, and H. Ezzaouia, "Crystal Growth of RuS 2 Using a Chemical Vapor Transport Technique and Its Properties," *Crystals*, vol. 12, no. 7, p. 994, 2022.

[72] A. Ubaldini and E. Giannini, "Improved chemical vapor transport growth of transition metal dichalcogenides," *Journal of Crystal Growth*, vol. 401, pp. 878–882, 2014.

[73] D. Wang, F. Luo, M. Lu, X. Xie, L. Huang, and W. Huang, "Chemical vapor transport reactions for synthesizing layered materials and their 2D counterparts," *Small*, vol. 15, no. 40, p. 1804404, 2019.

[74] T. Zhang *et al.*, "Creation of Magnetic Skyrmions in Two-Dimensional Van Der Waals Ferromagnets by Lattice Distortion," *Available at SSRN 5189861*.

[75] Z. Li *et al.*, "Room-temperature sub-100 nm Néel-type skyrmions in non-stoichiometric van der Waals ferromagnet Fe3-x GaTe2 with ultrafast laser writability," *Nature Communications*, vol. 15, no. 1, p. 1017, 2024.

[76] G. Hu *et al.*, "Room-Temperature Antisymmetric Magnetoresistance in van der Waals Ferromagnet Fe3GaTe2 Nanosheets," *Advanced Materials*, vol. 36, no. 27, p. 2403154, 2024.

doi:10.6342/NTU202503490

[77] S. Yao, T. Li, C. Yue, X. Xu, B. Zhang, and C. Zhang, "Controllable growth of centimetre-sized UTe 2 single crystals by the chemical vapor transport method," *CrystEngComm,* vol. 24, no. 35, pp. 6262–6268, 2022.

[78] G. Zhang *et al.*, "Above-room-temperature strong intrinsic ferromagnetism in 2D van der Waals Fe3GaTe2 with large perpendicular magnetic anisotropy," *Nature communications,* vol. 13, no. 1, p. 5067, 2022.

[79] H. Lim, H.-B. Ahn, and C. Lee, "Magnetic properties of ferromagnetic nanoparticles of Fe x GeTe2 (x= 3, 5) directly exfoliated and dispersed in pure water," *Nanotechnology,* vol. 35, no. 39, p. 395604, 2024.

[80] C. Liu, S. Zhang, H. Hao, H. Algaidi, Y. Ma, and X. X. Zhang, "Magnetic skyrmions above room temperature in a van der Waals ferromagnet Fe3GaTe2," *Advanced Materials,* vol. 36, no. 18, p. 2311022, 2024.

[81] M. Alghamdi *et al.*, "Highly efficient spin–orbit torque and switching of layered ferromagnet Fe3GeTe2," *Nano letters,* vol. 19, no. 7, pp. 4400–4405, 2019.

[82] X. Chen *et al.*, "Lattice Dynamics and Phonon Dispersion of the van der Waals Layered Ferromagnet Fe3GaTe2," *Nano Letters,* vol. 25, no. 11, pp. 4353–4360, 2025.

[83] F. M. Oliveira, N. Antonatos, V. Mazánek, D. Sedmidubský, Z. Sofer, and R. Gusmão, "Exfoliated Fe3GeTe2 and Ni3GeTe2 materials as water splitting electrocatalysts," *FlatChem,* vol. 32, p. 100334, 2022.

[84] A. A. Rezaie, E. Lee, D. Luong, J. A. Yapo, and B. P. Fokwa, "Abundant active sites on the basal plane and edges of layered van der Waals Fe3GeTe2 for highly efficient hydrogen evolution," *ACS Materials Letters,* vol. 3, no. 4, pp. 313–319, 2021.

doi:10.6342/NTU202503490

[85] R. Raman *et al.*, "Selective activation of MoS 2 grain boundaries for enhanced electrochemical activity," *Nanoscale Horizons*, vol. 9, no. 6, pp. 946–955, 2024.

[86] T. F. Jaramillo, K. P. Jørgensen, J. Bonde, J. H. Nielsen, S. Horch, and I. Chorkendorff, "Identification of active edge sites for electrochemical H2 evolution from MoS2 nanocatalysts," *science*, vol. 317, no. 5834, pp. 100–102, 2007.

[87] D. Voiry *et al.*, "Enhanced catalytic activity in strained chemically exfoliated WS2 nanosheets for hydrogen evolution," *Nature materials*, vol. 12, no. 9, pp. 850–855, 2013.

[88] J. Lee and J. H. Bang, "Reliable counter electrodes for the hydrogen evolution reaction in acidic media," *ACS Energy Letters*, vol. 5, no. 8, pp. 2706–2710, 2020.

[89] Z. Cui and W. Sheng, "Thoughts about choosing a proper counter electrode," *ACS Catalysis*, vol. 13, no. 4, pp. 2534–2541, 2023.

[90] A. J. Bard, L. R. Faulkner, and H. S. White, *Electrochemical methods: fundamentals and applications*. John Wiley & Sons, 2022.

[91] J. Wang and J. Schultze, "Analytical electrochemistry," *Angewandte Chemie-English Edition*, vol. 35, no. 17, pp. 1998–1998, 1996.

[92] R. G. Compton and C. E. Banks, *Understanding voltammetry*. World Scientific, 2007.

[93] J. Muthu, F. Khurshid, H.-T. Chin, Y.-C. Yao, Y.-P. Hsieh, and M. Hofmann, "The HER performance of 2D materials is underestimated without morphology correction," *Chemical Engineering Journal*, vol. 465, p. 142852, 2023.

[94] Y. Li, H. Wang, L. Xie, Y. Liang, G. Hong, and H. Dai, "MoS2 nanoparticles grown on graphene: an advanced catalyst for the hydrogen evolution reaction," *Journal of the American Chemical Society*, vol. 133, no. 19, pp. 7296–7299, 2011.

doi:10.6342/NTU202503490

[95] G. Kresse and J. Furthmüller, "Efficient iterative schemes for ab initio total-energy calculations using a plane-wave basis set," *Physical review B,* vol. 54, no. 16, p. 11169, 1996.

[96] J. P. Perdew, K. Burke, and M. Ernzerhof, "Generalized gradient approximation made simple," *Physical review letters,* vol. 77, no. 18, p. 3865, 1996.

[97] D. Voiry *et al.*, "Conducting MoS2 nanosheets as catalysts for hydrogen evolution reaction," *Nano letters,* vol. 13, no. 12, pp. 6222–6227, 2013.

[98] A. Ševčík, "Oscillographic polarography with periodical triangular voltage," *Collection of Czechoslovak Chemical Communications,* vol. 13, pp. 349–377, 1948.

[99] P. R. Bueno, "Nanoscale origins of super-capacitance phenomena," *Journal of Power Sources,* vol. 414, pp. 420–434, 2019.

[100] T. Binninger, "First-principles theory of electrochemical capacitance," *Electrochimica Acta,* vol. 444, p. 142016, 2023.

[101] D. M. Morales and M. Risch, "Seven steps to reliable cyclic voltammetry measurements for the determination of double layer capacitance," *Journal of Physics: Energy,* vol. 3, no. 3, p. 034013, 2021.

[102] N. Elgrishi, K. J. Rountree, B. D. McCarthy, E. S. Rountree, T. T. Eisenhart, and J. L. Dempsey, "A practical beginner's guide to cyclic voltammetry," *Journal of chemical education,* vol. 95, no. 2, pp. 197–206, 2018.

[103] T. Williams, R. Fuller, C. Vann, and D. Rappleye, "Semi-differentiation of reversible, soluble-insoluble potential sweep voltammograms," *Journal of The Electrochemical Society,* vol. 170, no. 4, p. 042502, 2023.

doi:10.6342/NTU202503490

[104] M. Pałys, T. Korba, M. Bos, and W. E. van der Linden, "The separation of overlapping peaks in cyclic voltammetry by means of semi-differential transformation," *Talanta*, vol. 38, no. 7, pp. 723–733, 1991.

[105] J. M. a. Pedrosa, M. a. T. Martín, J. J. Ruiz, and L. Camacho, "Application of the cyclic semi-integral voltammetry and cyclic semi-differential voltammetry to the determination of the reduction mechanism of a Ni–porphyrin," *Journal of Electroanalytical Chemistry*, vol. 523, no. 1-2, pp. 160–168, 2002.

[106] M. Kumar, F. Cervantes-Lee, K. H. Pannell, and J. Shao, "Synthesis and Cyclic Voltammetric Studies of the Diiron Complexes ER2 [(η5-C5H4) Fe (L2) Me] 2 (E= C, Si, Ge, Sn; R= H, alkyl; L2= diphosphine) and (η5-C5H5) Fe (L2) ER2Fc (Fc=(η5-C5H4) Fe (η5-C5H5))," *Organometallics*, vol. 27, no. 18, pp. 4739–4748, 2008.

[107] S. Favero *et al.*, "Same FeN4 Active Site, Different Activity: How Redox Peaks Control Oxygen Reduction on Fe Macrocycles," *ACS Electrochemistry*, 2025.

[108] E. Rudnik and P. Biskup, "Electrochemical behavior of tellurium in acidic nitrate solutions," *Metallurgy and Foundry Engineering*, vol. 40, pp. 15–31, 2014.

[109] J. Randles, "A cathode ray polarograph," *Transactions of the Faraday Society*, vol. 44, pp. 322–327, 1948.

[110] C.-W. Ahn *et al.*, "Self-growth of centimeter-scale single crystals by normal sintering process in modified potassium sodium niobate ceramics," *Scientific reports*, vol. 5, no. 1, p. 17656, 2015.

[111] E. Laviron, "General expression of the linear potential sweep voltammogram in the case of diffusionless electrochemical systems," *Journal of Electroanalytical Chemistry and Interfacial Electrochemistry*, vol. 101, no. 1, pp. 19–28, 1979.

doi:10.6342/NTU202503490

[112] K. J. Aoki, J. Chen, Y. Liu, and B. Jia, "Peak potential shift of fast cyclic voltammograms owing to capacitance of redox reactions," *Journal of Electroanalytical Chemistry*, vol. 856, p. 113609, 2020.

[113] C.-Y. Huang *et al.*, "In Situ Identification of Spin Magnetic Effect on Oxygen Evolution Reaction Unveiled by X-ray Emission Spectroscopy," *Journal of the American Chemical Society*, vol. 147, no. 16, pp. 13286–13295, 2025.

[114] S. Anjum, R. Tufail, K. Rashid, R. Zia, and S. Riaz, "Effect of cobalt doping on crystallinity, stability, magnetic and optical properties of magnetic iron oxide nano-particles," *Journal of Magnetism and Magnetic Materials*, vol. 432, pp. 198–207, 2017.

[115] L. Li, Y. Wang, R. R. Nazmutdinov, R. R. Zairov, Q. Shao, and J. Lu, "Magnetic field enhanced cobalt iridium alloy catalyst for acidic oxygen evolution reaction," *Nano Letters*, vol. 24, no. 20, pp. 6148–6157, 2024.

doi:10.6342/NTU202503490